Advances in Ecological Research, Volume 37, 2005, 101-141

Nonlinear stochastic population dynamics:

The flour beetle *Tribolium* as an effective tool of discovery

R. F. Costantino, Robert A. Desharnais, J. M. Cushing, Brian Dennis,

Shandelle M. Henson, and Aaron A. King

> When observation and theory collide, scientists turn to carefully designed experiments for resolution. Their motivation is especially high in the case of biological systems, which are typically far too complex to be grasped by observation and theory alone. The best procedure, as in the rest of science, is first to simplify the system, then to hold it more or less constant while varying the important parameters one or two at a time to see what happens.
>
> —Edward O. Wilson (2002)

INTRODUCTION

Prior to the seminal work of R. M. May in the 1970s, the prevailing paradigm viewed the unpredictable fluctuations in population time series data as random effects due to environmental variability and/or measurement errors. In the absence of environmental variability, according to this view, population numbers would either equilibrate or settle into regular periodic oscillations. May's (1974) suggestion that simple deterministic rules might explain the complex fluctuations observed in animal abundances led to an intense search for chaos in extant population data. The results of the search were suggestive, but

equivocal, and May's hypothesis remained the subject of lively debate (Zimmer 1999, Perry *et al*. 2000).

We took a different approach. Our interdisciplinary research team composed of statisticians, mathematicians, and biologists came together in the early 1990's to document *experimentally* the occurrence of nonlinear dynamic phenomena in biological populations. We began with the idea that nonlinear theory yields testable hypotheses concerning changes in the dynamical behaviors of populations. For example, in the case of the quadratic map (sometimes called the "logistic" map), changes in the intrinsic growth rate lead to a sequence of dynamical behaviors from equilibria to periodic cycles, to aperiodic chaotic behavior. Our thought was that a sequence of changes in dynamical behavior, which is a common feature of nonlinear models, could, in principle, be tested under controlled laboratory conditions. This would provide a connection between theory and data that was missing from ecology.

From the very beginning of our collaboration, fundamental questions greeted us at every turn as we looked at historical time series data and at data collected in our laboratories. Over the years we struggled to combine deterministic concepts such as equilibria, cycles, saddle nodes, bifurcations, basins of attraction, multiple attractors, resonance, and chaos with observations. What would a stable equilibrium, let alone chaos, look like in a population? Could a saddle node be invoked as an explanation for different transient behaviors of time series among replicate populations? Is chaos even possible if we consider discrete-state population models? Is it useful to consider populations as discrete-state stochastic systems?

In ecological theory, a central (and abiding) problem is to situate deterministic theory in the context of biological systems where important demographic events are probabilistic. Chance variation, in such fundamental biological processes as the number of offspring per adult and the chance of an individual surviving to adulthood, is a part of population dynamics. Probabilistic variation enters the overall research effort in the statistical methods associated with model identification, parameter estimation, and model validation. Chance events are also a component of the interpretation of population behavior; probabilistic variation is essential to the explanation of ecological time series data. We expand on these points.

First, a mathematical population model, built and tested as a serious scientific hypothesis, must be somehow connected to data. A probabilistic version of the model must be constructed to account for inevitable deviations of data from the predictions of the deterministic model. Demographic/environmental variability must be modeled in order to construct an appropriate estimating function for the model parameters (based on the likelihood or conditional sums of squares, for instance). Statistical diagnostic procedures should be used to evaluate the uncertainty component of the model.

Second, chance events interact with deterministic forces to produce emergent dynamic behaviors. The deterministic skeleton fixes the geometry of state space, providing a stage for the transient dance of stochasticity. Chance events allow the system to visit (and re-visit) the various deterministic entities on the stage, including unstable invariant sets, which under strict deterministic theory would have little or no impact on population time-series. Ecological time-series can display a stochastic mix of many of the dynamic features of the skeleton, including multiple attractors, transients, unstable

invariant sets (such as saddles and unstable manifolds) and lattice effects. Stochasticity enlarges the repertoire of time series orbits; each population, even in a set of laboratory replicates, may display a unique sequence of population abundances.

In this chapter, we expand upon the message that in order to understand population fluctuations, deterministic *and* stochastic forces must be viewed as an integral part of the ecological system. We begin by laying out our models, animal and mathematical. We then discuss how we estimated model parameters and validated the model. Next, with the parameterized model in hand, we present an overview of some of the nonlinear phenomena and related topics that we have documented in our experimental system: chaotic dynamics, population outbreaks, saddle nodes, phase switching, lattice effects, the anatomy of chaos, and finally, mechanistic models of stochasticity.

ANIMAL MODEL

Our experience with the flour beetle *Tribolium castaneum* (Herbst) made it our choice as the animal model (Costantino and Desharnais 1991). Nevertheless, in the spring of 1992, it was far from clear that the beetle system would meet the demands for an in-depth investigation of nonlinear population dynamics. Several features made the beetle attractive. Much of the biology is understood and the life cycle is sufficiently complicated that the dynamical possibilities are rich; moreover, there is a consensus that cannibalism plays a major role in beetle dynamics (Mertz 1972). Laboratory protocols to culture and manipulate the insects in a controlled setting are well established. Bi-weekly census counts can be accurate and can be taken over many reproductive cycles in a relatively short period of time. The animals are routinely cultured in half-pint milk bottles

containing 20g of standard medium, in incubators maintained at a constant temperature, relative humidity and amount of light. In general, environmental variation is minimized. However, environmental variability can be imposed on the system, for example, by altering the size of the habitat following a census.

DETERMINISTIC SKELETON

Small. That was the word of caution for building the model. Keep the number of parameters small. Keep the number of state variables small. A model with an over abundance of parameters and state variables (relative to the amount of data available) will be difficult to analyze mathematically and impossible to test statistically.

To construct the mathematical model, we proposed deterministic equations for the prediction of measurable state variables from one census time to the next. The state variables were chosen to be the numbers of larvae, L, pupae, P, and adult beetles, A. The resulting larval-pupal-adult (LPA) model is a system of three difference equations. The deterministic LPA model predicts the numbers of animals in each stage at time $t + 1$ given the actual number of animals in each stage at time t:

$$\begin{aligned} L_{t+1} &= bA_t \exp\left(-\frac{c_{ea}}{V} A_t - \frac{c_{el}}{V} L_t \right), \\ P_{t+1} &= (1-\mu_l) L_t, \\ A_{t+1} &= P_t \exp\left(-\frac{c_{pa}}{V} A_t \right) + (1-\mu_a) A_t. \end{aligned} \tag{1}$$

Here L_t is the number of feeding larvae at time t, P_t is the number of non-feeding larvae, pupae and callow adults at time t, and A_t is the number of sexually mature adults at time t. The unit of time is two weeks, which is the approximate amount of time spent in each of

the L and P classes under experimental conditions. The average number of larvae recruited per adult per unit time in the absence of cannibalism is $b > 0$, and the fractions μ_a and μ_l are the adult and larval probabilities of dying from causes other than cannibalism in one time unit. In *T. castaneum*, larvae and adults eat eggs and adults eat pupae. The exponential expressions represent the fractions of individuals surviving cannibalism in one unit of time, with cannibalism coefficients $c_{ea}/V, c_{el}/V, c_{pa}/V > 0$. Habitat size V has units equal to the volume occupied by 20g of flour, the amount of medium routinely used in our laboratory.

STOCHASTIC MODELS

The LPA model (1) is not complete. The model must include a probabilistic portion that specifies how the variability in the data arose. There are many ways of formulating a stochastic model. We present two possibilities.

Ecologists have drawn a distinction between environmental stochasticity (chance variation from extrinsic sources affecting many individuals) and demographic stochasticity (intrinsic chance variation in individual births and deaths) in populations (May 1974, Shaffer 1981, Simberloff 1988). Environmental noise can be modeled as being additive on the log scale, while demographic noise is additive on the square root scale (Dennis *et al.* 1995, 2001).

In our early explorations of the LPA model we used an environmental stochastic version (2) to describe the dynamics of larvae, pupae and adults (Dennis *et al*. 1995):

$$
\begin{aligned}
L_{t+1} &= bA_t \exp\left(-\frac{c_{ea}}{V} A_t - \frac{c_{el}}{V} L_t + E_{1t}\right), \\
P_{t+1} &= (1-\mu_l) L_t \exp(E_{2t}), \\
A_{t+1} &= \left(P_t \exp\left(-\frac{c_{pa}}{V} A_t\right) + (1-\mu_a) A_t\right) \exp(E_{3t}).
\end{aligned} \tag{2}
$$

Later experiments and analyses supported a demographic stochastic LPA model (3) (Dennis *et al.* 2001):

$$
\begin{aligned}
L_{t+1} &= \left[\sqrt{bA_t \exp\left(-\frac{c_{ea}}{V} A_t - \frac{c_{el}}{V} L_t\right)} + E_{1t}\right]^2, \\
P_{t+1} &= \left[\sqrt{(1-\mu_l) L_t} + E_{2t}\right]^2, \\
A_{t+1} &= \left[\sqrt{P_t \exp\left(-\frac{c_{pa}}{V} A_t\right) + (1-\mu_a) A_t} + E_{3t}\right]^2.
\end{aligned} \tag{3}
$$

In models (2) and (3), $\boldsymbol{E}_t = [E_{1t}, E_{2t}, E_{3t}]'$ is a random vector and is assumed to have a trivariate normal distribution with a mean vector of $\mathbf{0}$ and a variance-covariance matrix of $\boldsymbol{\Sigma}$. Covariances among E_{1t}, E_{2t}, and E_{3t} at any given time t are assumed (and represented by off-diagonal elements of $\boldsymbol{\Sigma}$), but we expect the covariances between times to be small by comparison. Thus we assume that $\boldsymbol{E}_0$, $\boldsymbol{E}_1$, ... are uncorrelated. In rare instances where a large negative E_{it} causes the term in square brackets to be negative, the value of that life stage is set to zero.

PARAMETER ESTIMATION AND MODEL VALIDATION

A mathematical model is a scientific hypothesis expressed in the peculiarly precise, quantitative language of mathematics. How is the hypothesis to be evaluated? How are

model parameters to be estimated? How is a statistical test of the model constructed? To what extent can the precision of the mathematical model be translated into strong statistical tests? More generally, how are theory and data to be joined? Finding working solutions to these problems have been an important feature of our research effort.

The stochastic construction represented by models (2) and (3) have a number of statistical advantages. First, written on the logarithmic scale for (2) and on the square root scale for (3), the stochastic models are seen to be a type of multivariate, nonlinear, autoregressive (NLAR) model:

$$\boldsymbol{W}_{t+1} = \boldsymbol{h}\left(\boldsymbol{W}_t\right) + \boldsymbol{E}_t .$$

Here $\boldsymbol{W}_t$ is the column vector of the logarithmic-transformed state variables, $\boldsymbol{W}_t = [\ln L_t, \ln P_t, \ln A_t]'$, or square root-transformed, $\boldsymbol{W}_t = [\sqrt{L_t}, \sqrt{P_t}, \sqrt{A_t}]'$, state variables; $\boldsymbol{h}(\boldsymbol{W}_t) = [g\{bA_t \exp(-\left(c_{ea}/V\right) A_t - \left(c_{el}/V\right) L_t\},\ g\{1-\mu_l)L_t\},$ $g\{P_t \exp(-\left(c_{pa}/V\right) A_t + (1-\mu_a) A_t\}]'$ is a column vector of functions (where $g(\cdot)$ is either a logarithmic or square root transformation); and $\boldsymbol{E}_t$ has a multivariate normal ($\mathbf{0}$, $\boldsymbol{\Sigma}$) distribution. Development of statistical methods (estimation, testing, and evaluation) for NLAR models has received much attention (Tong 1990). Second, this stochastic construction preserves the dynamical properties of the deterministic model (1) through one-step predictions (conditional expected values). Third, changes in the underlying deterministic forms can easily be accommodated in the stochastic construction. Fourth, the model is easy to simulate and, finally, parameter estimates are straightforward to compute.

The stochastic construction has biological advantages as well. The models allow for covariance of fluctuations in larvae, pupae, and adults in a given time period, as described by the covariance of elements in $\boldsymbol{E}_t$. Autocovariances of the noise elements through time, though, are not expected to be important compared to the covariances between the elements within a time, provided the underlying dynamics (deterministic skeleton) are specified correctly. The different scales of variability for larvae, pupae, and adults are accounted for through the parameters on the main diagonal of the variance-covariance matrix $\boldsymbol{\Sigma}$.

The stochastic LPA models (2) and (3) provide an explicit likelihood function. A likelihood function gives the probability, under the proposed stochastic model, that the random outcome would be the observed time series. A likelihood function is a fundamental tool in statistical inference (Stuart and Ord 1991) and represents the crucial connection between data and model. Data for a particular *Tribolium* population are a realization of the joint stochastic variables $L_t, P_t,$ and A_t. The data take the form of a trivariate time series: $(l_0, p_0, a_0), (l_1, p_1, a_1), \cdots, (l_q, p_q, a_q)$. Let $\boldsymbol{w}_t$ denote the column vector of transformed observations at time t: $\boldsymbol{w}_t = [\ln l_t, \ln p_t, \ln a_t]'$ or $\boldsymbol{w}_t = [\sqrt{l_t}, \sqrt{p_t}, \sqrt{a_t}]'$. Suppose $\boldsymbol{\theta}$ denotes the unknown parameters in the functions in $\boldsymbol{h}(\cdot)$, i.e., the parameters in the deterministic model equations. Additional unknown parameters are in the variance-covariance matrix $\boldsymbol{\Sigma}$. The likelihood function $L(\boldsymbol{\theta}, \boldsymbol{\Sigma})$ is given by

$$L(\boldsymbol{\theta}, \boldsymbol{\Sigma}) = \prod_{t=1}^{q} p(\boldsymbol{w}_t \,|\, \boldsymbol{w}_{t-1}),$$

where $p(\boldsymbol{w}_t | \boldsymbol{w}_{t-1})$ is the joint transition probability density function, that is, the joint probability density function for $\boldsymbol{W}_t$ conditional on $\boldsymbol{W}_{t-1} = \boldsymbol{w}_{t-1}$ and evaluated at $\boldsymbol{w}_t$ .The maximum likelihood (ML) estimates of parameters in $\boldsymbol{\theta}$ and $\boldsymbol{\Sigma}$ are those values that jointly maximize $L(\boldsymbol{\theta}, \boldsymbol{\Sigma})$, or, equivalently, $\ln L(\boldsymbol{\theta}, \boldsymbol{\Sigma})$. The ML estimates of parameters in $\boldsymbol{\theta}$ must be obtained numerically for any particular data set. We have found that maximizing the log-likelihood using the Nelder-Mead simplex algorithm is convenient, reliable, and easy to program (Olsson and Nelson 1975, Press *et al*. 1986). ML estimates for the stochastic LPA models have desirable statistical properties. ML estimates are asymptotically unbiased, asymptotically efficient, and asymptotically normally distributed. However, the properties of ML estimates do not hold if the model is a poor description of the underlying stochastic mechanisms producing the data. In particular, if the noise vector $\boldsymbol{E}_t$ does not have a multivariate normal distribution, or is correlated through time, then the ML estimates could be biased. Since we aim to identify dynamic behavior by estimating where the parameters in $\boldsymbol{\theta}$ are in parameter space, an alternative estimation method that yields more robust parameter estimates is useful.

The method of conditional least squares (CLS) was also used for estimation of the parameters. CLS methods relax many distributional assumptions about the noise variables in the vector $\boldsymbol{E}_t$ (Klimko and Nelson 1978, Tong 1990). CLS estimates are consistent (converge to the true parameters as sample size increases), even if $\boldsymbol{E}_t$ is non-normal and autocorrelated, provided the stochastic model has a stationary distribution. In the LPA model, CLS estimates reduce to three univariate cases because any given parameter does not appear in more than one model equation. CLS estimates are based on the sum of squared differences between the value of the variable observed at time t and

its expected (or one-step forecast) value, given the observed state of the system at time $t-1$. For the LPA model, there are three such conditional sums of squares:

$$Q_1(\boldsymbol{\theta}_1) = \sum_{t=1}^{q} \left\{ g(l_t) - g\left[b a_{t-1} \exp\left(-\frac{c_{ea}}{V} a_{t-1} - \frac{c_{el}}{V} l_{t-1} \right) \right] \right\}^2 ,$$

$$Q_2(\theta_2) = \sum_{t=1}^{q} \left\{ g(p_t) - g\left[(1-\mu_l) l_{t-1} \right] \right\}^2 ,$$

$$Q_3(\boldsymbol{\theta}_3) = \sum_{t=1}^{q} \left\{ g(a_t) - g\left[p_{t-1} \exp(-\frac{c_{pa}}{V} a_{t-1}) + (1-\mu_a) a_{t-1} \right] \right\}^2 .$$

Here $\boldsymbol{\theta}_1 = \left[b, c_{el}, c_{ea} \right]'$, $\theta_2 = \mu_l$, and $\boldsymbol{\theta}_3 = \left[c_{pa}, \mu_a \right]'$ are the parameter vectors from the model equations. The conditional sums of squares are constructed on the logarithmic or square root scales because that is the scale on which we assume noise is additive. Three separate numerical minimizations are required, one for each of the above sums of squares. We find the Nelder-Mead simplex algorithm convenient. The estimates of the parameters in the variance-covariance matrix of $\boldsymbol{E}_t$ are then found from the sums of squares and cross products matrix constructed using the conditional residuals.

Model evaluation procedures center on the residuals defined as the differences of the logarithmic (or square root) state variables and their one-step (estimated) expected values:

$$\boldsymbol{e}_t = \boldsymbol{w}_t - \hat{\boldsymbol{h}}(\boldsymbol{w}_{t-1}).$$

Here $\boldsymbol{e}_t$ is a vector of residuals for $g(l_t), g(p_t), g(a_t)$ in a population at time t, and $\hat{\boldsymbol{h}}$ denotes the functions in $\boldsymbol{h}$ evaluated at the ML parameter estimates. If the model fits,

then $\boldsymbol{e}_1, \boldsymbol{e}_2, ..., \boldsymbol{e}_q$ should behave approximately like uncorrelated observations from a trivariate normal distribution. Departures of the residuals from normality can be investigated using graphical procedures such as quantile-quantile plots and tested using the Lin-Mudholkar statistic (Tong 1990). Autocorrelations of residuals indicates a relationship between successive prediction errors and thus might suggest a systematic lack of fit between model and data. First and second (or higher) order autocorrelations of residuals can be computed and tested for significance.

In Dennis *et al*. (1995), we applied a maximum likelihood procedure to the data of Desharnais and Costantino (1980) and conducted rigorous diagnostics for the evaluation of the stochastic model (2). A single set of parameter values from the control cultures was able to describe the dynamics of nine demographically manipulated cultures, even though none of the data from these manipulated populations were used to obtain the parameter estimates. The observed time series for a representative replicate together with the one-step predictions are graphed in Fig. 1. The solid lines connect the observed census data (closed circles). Dashed lines connect the observed numbers at time t with the forecast (open circles) at time $t+1$. The accuracy of a particular forecast can be judged by comparing the predictions at time $t+1$ with the number of animals actually observed at time $t+1$. In general, the graph reveals a close association between the one-step forecast and the census data. Parameter estimation placed the population in the region of parameter space that corresponds to stable 2-cycles of the deterministic skeleton of the LPA model.

Similar statistical methods for parameter estimation and model validation were applied to the data from two other experiments described in this chapter (Dennis *et al*.

1997, 2001). In both cases, the diagnostic analyses of the residuals supported the LPA model.

EXPERIMENTAL CONFIRMATION OF NONLINEAR DYNAMIC PHENOMENA

The laboratory system—beetles in a bottle together with the deterministic and stochastic models—was devised to test basic ecological hypotheses in isolation from confounding factors. With a parameterized and validated model for laboratory cultures of *T. castaneum* in hand, we were ready to open a new phase of our research in which experiments are focused directly on phenomena such as bifurcation sequences, equilibria, cycles, stable and unstable manifolds, and chaos.

Recognizing that we are part of a continuing tradition of using flour beetles in ecological research it seems appropriate to recall the philosophy of laboratory research stated 50 years ago by pioneering ecologist Thomas Park (1955):

> Research in laboratory population ecology should take its orientation from some phenomenon known or suspected to occur in nature and known or suspected to have significant ecological consequences. Its objective is not to erect an indoor ecology but, rather, to illustrate conceptually the general problem to which it is addressed. The research is thus the handmaiden of field investigation; not the substitute. Findings derived from such studies are *models* of selected events in natural environments. The models, though not simple, are simplified; they are under a regimen of planned control, and their intrinsic interactions are likely to be intensified. To this extent

they are unrealistic. But they remain, nonetheless, quantitative *biological* models and their unrealistic aspects may be a virtue instead of a vice. This is to say, they can contribute to the maturation of ecology, at least until that time when they are no longer needed.

We begin our presentation of selected nonlinear phenomena documented in our laboratories by describing an experiment based on a model predicted sequence of transitions in dynamic behavior occurring in response to changes in the adult death rate.

BIFURCATIONS IN THE DYNAMIC BEHAVIOR OF POPULATIONS

Nonlinear mathematical models can undergo sudden transitions in dynamic behavior in response to changes in parameter values. Specifically, the long term attractors of model trajectories—stable points, stable cycles, loops, strange attractors—can exhibit abrupt changes in identity and stability when model parameter values are altered. The anatomy and taxonomy of these changes is the focus of bifurcation theory in nonlinear dynamics.

An important biological point is that a given nonlinear model may forecast a unique parade of dynamic behaviors in response to parameter change. If a population rate quantity—birth rate, death rate, migration rate, etc.—could be manipulated experimentally, the resulting observed population responses would serve as a test of the model bifurcation sequence.

The LPA model predicts such a sequence of transitions in dynamic behavior in response to changing values of the adult death rate parameter μ_a. A bifurcation (or final-state) diagram is a plot of the asymptotic dynamical behaviors as a function of adult

mortality (Fig. 2). For very small values of mortality there is a stable fixed point. As μ_a increases a period doubling bifurcation to stable 2-cycles occurs. With further increases in μ_a there occurs a surprising reversal to an interval of stable equilibria. An increase of μ_a to values near one results in another destabilization of equilibria and, in this case, a bifurcation to invariant loop attractors in phase space and quasi-periodic time series (called a Neimark-Sacker bifurcation).

To test the bifurcation prediction we manipulated adult mortality rate in beetle cultures (Costantino *et al*. 1995; Dennis *et al*. 1997). Rigorous statistical verification of the predicted shifts in dynamical behavior provided convincing evidence that the observed transitional changes did indeed correspond to those forecast by the mathematical model (see Fig. 3).

A SECOND BIFURCATION EXPERIMENT: THE HUNT FOR CHAOS

Ecologists searched for chaos in historical data. This involved various statistical methods for the analysis of existing time series (e.g. Ellner and Turchin 1995, Turchin and Ellner 2000, Perry *et al*. 2000). Our approach was experimental. We focused not on a particular time series but rather on a collection of time series taken from treatments designed to lie along a route to chaos. Thus, any claim that chaotic dynamics influenced the populations would not rest on a single data set, but would be supported by the dynamics observed across an entire sequence of predicted bifurcations.

Thus, our hunt for chaos took the form of a second transitions experiment whose protocol was based upon an LPA-model-predicted sequence of bifurcations (Costantino *et al*. 1997). This sequence occurs in the model when the adult death rate is $\mu_a = 0.96$

and the adult cannibalism of pupae c_{pa} is increased (by manipulating adult recruitment). The sequence (see Fig. 4) begins at $c_{pa} = 0$ with quasi-periodic oscillations around an invariant loop. With further increases in c_{pa} the predicted dynamics pass through a complicated array of aperiodic attractors and period locking windows (where the motion around the loop is exactly periodic) until finally chaotic and strange attractors dominate. For sufficiently large values of c_{pa} there is predicted a distinctive cycle of period three which bifurcates to a six-cycle near $c_{pa} = 1$.

Based on these predictions, the "hunt for chaos experiment" was designed with adult mortality rate at $\mu_a = 0.96$. The adult recruitment rate was manipulated so that it would equal $P_t \exp(-c_{pa} A_t)$, with values of c_{pa} set at 0.00, 0.05, 0.10, 0.25, 0.35, 0.50, and 1.00. There was also an unmanipulated control treatment.

The data from these experiments, together with the predicted deterministic attractors and stochastic realizations of model (3) using the estimated parameter values, are plotted in phase space in Fig. 5. The pattern of changes in dynamics and variability from treatment to treatment are well-captured by the model, from the stable point equilibrium of the control, to the irregular behavior of $c_{pa} = 0.35$, to the strong periodic signals in the $c_{pa} = 0.50$ and 1.00 treatments.

These results illustrate two important messages. Biological systems can undergo transitions between different types of deterministic behaviors in response to changing conditions. Moreover, these transitions might be predictable by means of suitable stochastic versions of the models (Dennis *et al*. 2001).

CHAOS AND POPULATION OUTBREAKS

Sensitivity to initial conditions is a key characteristic of chaos. This property led to suggestions on how small perturbations might be used to influence the dynamics of chaotic systems. One idea is that by "nudging" the parameters or state variables at points in the trajectory where the system is particularly sensitive to perturbations, one might produce a desired effect, large relative to the perturbation applied. Several authors discuss this method for population control in ecology (Doebeli 1993; Solé *et al*. 1999; Shulenburger *et al*. 1999; Hawkins and Cornell 1999), but provide no experimental test of the procedure. In this section, we show how small demographic perturbations in adult numbers can be used to dampen large chaotic fluctuations in the densities of larvae (Desharnais *et al*. 2001).

The chaotic strange attractor for $\mu_a = 0.96$ and $c_{pa} = 0$ has regions of differing sensitivities to initial conditions (Fig. 6A). For each of 2000 points on the attractor we computed the three eigenvalues of the Jacobian matrix of the deterministic LPA model. Each point was shaded according to λ_t, the logarithm of largest modulus of the three eigenvalues: light gray for negative values, dark gray for moderate positive values, and black for large positive values. These numbers, which ranged from –1.03 to 3.92, are the local Liapunov exponents for one step in the orbit (Bailey *et al*. 1997). They measure the effect of small perturbations on the population trajectory. Values of $\lambda_t > 0$ indicate regions of phase space where nearby trajectories diverge in the next time step; values of $\lambda_t < 0$ occur in regions where nearby trajectories converge. The black coloration in Fig. 6A indicates a "hot" region of the attractor where larval and adult numbers are small and

numbers of pupae are large. Small perturbations in this region can have a large effect on the population.

We closely studied orbits of simulated populations and noticed that differences of a few adults in the "hot region" resulted in widely divergent trajectories. This led to the identification of two rules which we subsequently used in the experimental protocol. The first or "in-box" rule, which forecasts a reduction in larval numbers with small perturbations in the number of adult beetles, is as follows. If the life stage vector $[L_t, P_t, A_t]$ is such that $L_t \leq 150$ and $A_t \leq 3$ then three adults are added to the culture; otherwise no perturbation is made. We developed a second or "out-box" rule as a control to demonstrate that it is the dynamics associated with the "hot spots" on the chaotic attractor that are responsible for the reduction in larval numbers and not simply the fact that adults were added to the culture. Under this rule, if the life stage vector $[L_t, P_t, A_t]$ is such that $L_t > 150$ or $A_t > 3$ then three adults are added to the culture; otherwise no manipulation is made. The regions where the in-box and out-box perturbations are applied are represented in Fig. 6B.

We conducted an experimental evaluation of the predicted perturbation responses by establishing nine laboratory populations of the RR strain of the flour beetle *T. castaneum*. As in the study described in the previous section, we experimentally set the adult mortality rate at 0.96 and manipulated the adult recruitment rate so that it would equal $P_t \exp(-c_{pa} A_t)$ with $c_{pa} = 0.35$. Three of the populations formed an experimental control treatment where no perturbations were applied for the duration of the experiment. For the six remaining cultures, the above procedure was continued for 132 weeks; however, at week 134 and thereafter for a total of 78 weeks, in addition to manipulating

μ_a and c_{pa}, we applied the in-box perturbation rule to three populations and the out-box rule to three populations until week 210 after which we stopped the in-box and out-box perturbations and maintained the cultures for another 54 weeks.

Predicted and observed time series for larval numbers are shown in Fig. 7. The panels on the left side of the figure show realizations from the stochastic version of the LPA model (3) with parameters estimated from a previous study (Dennis *et al.* 2001). The panels on the right side are for one representative replicate population from each of the three experimental treatments. Both the simulated and observed populations in the unperturbed control treatment (Fig. 7A, B) show large chaotic fluctuations in larval numbers similar to those observed in previous studies (Costantino *et al*. 1997, Dennis *et al*. 2001). The in-box perturbations, which were designed to decrease the amplitude of the fluctuations in insect numbers, had the desired effect. The model and experimental populations in the in-box treatment exhibit large amplitude fluctuations prior to the in-box perturbations (solid symbols in Fig. 7C, D), but these oscillations dampened dramatically after the in-box perturbations were applied (open symbols in Fig. 7C, D). On the other hand, as predicted by the model, the out-box populations continued to exhibit large amplitude fluctuations in larval numbers during the out-box perturbations (Fig. 7E, F). This was despite the fact that, in accordance with the experimental protocol, the out-box perturbations were applied more often than the in-box perturbations. This demonstrates that the dampening effect of the in-box treatment was due to the timing of the perturbations to coincide with the occurrence of life stage numbers in a sensitive region of phase space (box in Fig. 6B). During the final 54 weeks of the experiment, the LPA model prediction was for the oscillatory amplitudes of the cultures to return to the

levels attained prior to the application of the perturbations. That behavior was observed (Fig. 7).

Can small perturbations be used to influence the dynamics of natural ecosystems? The question has yet to be addressed by field ecologists. Certainly introduction of a handful of individuals of a non-native species into a region can have wide ranging effects. However, the possibility of changing the dynamics of an abundant species in the field with small perturbations has not been explored to our knowledge. Here we have made the step from theoretical possibility to laboratory demonstration. For a similar approach to be effective in field populations, a model of the dynamics of the system is required which can be used to make accurate predictions. Such models will come from careful studies of the mechanisms that determine ecological change (Kendall *et al*. 1999, Perry *et al*. 2000, Turchin and Ellner 2000).

BACK IN THE SADDLE (NODE) AGAIN

Random events can frequently and repeatedly produce visits near *unstable* equilibria, cycles, or other invariant sets. Such visitations can result in the influence of unstable invariant sets on the dynamics of a population. This is particularly true for unstable invariant sets that are not repelling. In the higher dimensional systems typically found in ecology, unstable invariant sets often are associated with attracting regions in phase space; that is, there are points in phase space whose orbits approach the unstable set. These points constitute the "stable manifold" of the invariant set. Moreover, points near, but not on this stable manifold are temporarily drawn toward the unstable set before being repelled away towards an attractor. Unstable invariant sets of this type are called

"saddles". Nonlinear systems, particularly those with complex dynamics, are generally replete with saddles.

Since random events can cause deviations away from an attractor and place an orbit near an unstable set or its stable manifold, a population's dynamics becomes a mixture of influences from both stable and unstable sets. Indeed, the predicted stationary distribution of most stochastic models covers all (or most) of feasible phase space, and therefore such a mixture is theoretically certain to happen. The resulting temporal patterns are then a matter of the relative strengths of the influences due to the unstable and stable invariant sets.

Here we present evidence for the influence of a saddle observed in a replicate of the $c_{pa} = 0.05$ treatment of the hunt for chaos experiment. In Fig. 8 plots of the larval, pupal and adult time series of the deterministic model (1), stochastic realizations of model (3), and the data are presented. The deterministic time series displays no influence of the presence of the unstable equilibrium (Fig. 8A). The stochastic model forecasts that the time series of some stochastic realizations and some experimental orbits will visit the unstable equilibrium and remain relatively nonoscillatory at low levels before returning to the asymptotic stable attractor. One such stochastic realization is presented in Fig. 8B. A saddle fly-by occurs in the interval marked by the double ended arrow. The experimental data show a saddle fly-by in the interval from time step $t = 8$ to $t = 17$.

In the four panels of Fig. 9, the deterministic model-predicted invariant loop (black closed curve) and the data orbit (open symbols) are presented in phase space. In the first panel the data for time steps 0 to 8 (weeks 0 to 16) show a temporal motion around the loop. However, at time step 8 there is a perturbation away from the loop

which places the data point near the model predicted *unstable* equilibrium (solid circle). From time steps 8 to 13 (weeks 16 to 26) the data orbit stays clustered very near this predicted equilibrium. Indeed, if the interval of observation were restricted to the first 13 time steps of the experiment an inaccurate conclusion of equilibrium dynamics might be made. The equilibrium, however, is unstable and the data orbit, from time steps 13 to 19, displays a "star-like" rotational motion in state space as the data orbit leaves the vicinity of the saddle equilibrium and returns to the stable invariant loop. This geometrically distinctive path is predicted by the deterministic LPA model (1). The linearization at the equilibrium has a conjugate pair of complex eigenvalues $re^{\pm i\theta}$ of magnitude $r \approx 1.265 > 1$ and polar angle $\theta \approx 2.576$ (and a third real positive eigenvalue $\lambda \approx 0.3945 < 1$). This complex eigenvalue implies a rotational motion away from the saddle of approximately $2\pi/\theta \approx 2.439$ radians ($139.8°$) per step, the motion occurring approximately in a plane parallel to that spanned by the eigenvectors $(L, P, A) \approx (1, -1.116, 0.4860)$ and $(1, -0.3526, -0.2817)$. In the fourth panel the data return to the model predicted quasi-periodic motion around the invariant loop.

For the deterministic LPA model, only those time series whose orbits pass near the stable manifold will be strongly influenced by the saddle node. Moreover, once the population has reached the stable attractor it will stay there forever. This is true neither for stochastic LPA model time series nor for experimental observations. Chance events can cause a population to land near the stable manifold and come under the influence of the saddle node. This might even reoccur on several occasions in a time series, and several 'fly-bys' of the saddle would then be present in the data (Cushing *et al*. 2003).

The stochastic component of the dynamics can therefore account for different transient behaviors of time series in identically replicated experimental populations.

PHASE SWITCHING IN POPULATION CYCLES

Populations often exhibit temporal oscillations, and sometimes these oscillations shift phase. A common phenomenon observed in oscillating *Tribolium* cultures is a change of phase in which, for example, a high-low periodic pattern "chicken-steps" (skips) to a low-high pattern. Fig. 10A displays larval numbers for two of the control replicates from the experiments of Desharnais and Costantino (1980). The cultures, shown to be oscillating with period 2 (Dennis *et al*. 1995), display phase shifts in both replicates which eventually lead to asynchronous oscillations. Two other examples appear in Fig. 10, one from the experiment of Costantino *et al*. (1995) involving a two-cycle (Fig. 10B) and another from the experiment of Costantino *et al.* (1997)) involving a three-cycle (Fig. 10C).

We hypothesize that phase shifts correspond to stochastic jumps between basins of attraction in an appropriate phase space which associates the different phases of a periodic cycle with distinct attractors (Henson *et al*. 1998).

At the maximum likelihood LPA parameters estimated from the control replicates reported in Desharnais and Costantino (1980) the model admits an unstable fixed-point with coordinates (rounded to the nearest beetle)

$$[L, P, A] = [124, 60, 97]$$

This fixed point is stable in some directions and unstable in other directions; it is a saddle node as described in the previous section. The model also predicts two locally stable 2-cycle solutions: one which alternates between the stage vectors

$$[L, P, A] = [18,\ 158,\ 106]$$

$$[L, P, A] = [325,\ 9,\ 118]$$

and the other, which traverses the same vectors in opposite phase

$$[L, P, A] = [325,\ 9,\ 118]$$

$$[L, P, A] = [18,\ 158,\ 106].$$

Because they "live" on the same attractor {[18, 158,106], [325, 9, 118]}, the two different 2-cycles listed above are indistinguishable when plotted in phase space. However, these 2-cycles do determine different phases for each component. For example, the first cycle determines a low-high oscillation in the larval component, while the second determines a high-low oscillation in the larval component. In order to differentiate between these out-of-phase 2-cycles as separate attractors with distinct basins of attraction, we turn to the composite of the LPA model.

The "composite LPA model" (the composite map, whose solutions correspond to even time steps of solutions of the LPA model) identifies the above 2-cycles as two different fixed point attractors given by the stage vectors

$$[L, P, A]_{\Delta} = [18,\ 158,\ 106] \text{ and } [L, P, A]_{O} = [325, 9, 118].$$

(Note the subscripts Δ and O are used to label the two attractors.) The saddle point of the LPA map (labeled with the subscript +) is also a saddle point

$$[L, P, A]_{+} = [124,\ 60,\ 97]$$

of the composite map.

The basins of attraction of the two stable fixed points of the composite LPA model are sets in 3-dimensional phase space and are computed numerically. In this particular example, the basins are fairly simple sets. Throughout a large portion of phase space, they are separated by a 2-dimensional surface (containing the saddle) that forms part of the "basin boundary." Initial conditions on one side of the boundary lead to composite map solutions that approach $[L, P, A]_{\Delta}$, while initial conditions on the other side generate composite map solutions approaching $[L, P, A]_{O}$. Solutions starting on the basin boundary near the saddle point tend to the saddle $[L, P, A]_{+}$ (locally, the boundary is the "stable manifold" of the unstable saddle). Indeed, near the saddle, the stable manifold of this unstable entity forms the watershed geometrical feature of phase space. Near the origin, however, the basin boundary becomes much more complicated; but this will not concern us.

Deterministic and stochastic time series generated by the LPA model for the L-stage are displayed in Fig. 11 using the initial condition [70, 35, 64] of the experiment described above. The deterministic time series approaches the 2-cycle shown in Fig. 11A. In composite phase space, the corresponding solution of the composite LPA map approaches the fixed point $[L, P, A]_{\Delta}$ = [18, 158, 106] (Fig. 11D). The stochastic model L-stage time series, on the other hand, shifts phase at time t = 7 and again at t = 15 (Fig. 11B). In composite phase space, these phase changes occur exactly when the basin boundary is crossed (Fig. 11E). The data for replicate B from Desharnais and Costantino (1980) are shown in Fig. 11C and F. As the LPA model predicts, phase shifting occurs in

the data time series precisely when the data cross the model predicted basin boundary in composite phase space.

Deterministic attractors alone do not account for the phase shifting mechanism proposed. Indeed, in some situations attractors may be of little interest as final states. Other invariant sets such as basin boundaries and saddle points, along with stochasticity, play a key role, and may lead to data dominated by transient rather than asymptotic dynamics.

LATTICE EFFECTS

The discovery that simple deterministic population models can display complex aperiodic fluctuations such as chaos (May 1974) inspired decades of empirical and theoretical work in ecology (Hastings *et al*. 1993, Dennis *et al.* 2001). The resulting mathematical models of population dynamics almost invariably employ a continuous state space. That is, variables representing population densities in these models are real-valued. But animals, and for many practical purposes, plants, are individuals. More realistic models would therefore cast population densities as discrete variables, with state space a discrete lattice of numbers. As long as population size is bounded, deterministic models of the latter type have finitely many possible states and hence display only periodic cycles. In particular, discrete-state deterministic models with bounded dynamics cannot display chaos.

Approximating population size with continuous-state models is commonly justified by the assumption that population numbers remain so large that the discrete state space lattice is sufficiently fine (May 1974). However, the deterministic dynamics of associated discrete-state and continuous-state models can be quite different even for very

large population sizes, so that the effects caused by the discreteness of animal densities (*lattice effects*) cannot always be ignored (Jackson 1989).

As we have repeatedly emphasized, ecological systems are invariably stochastic. Discrete-state models, when perturbed by stochasticity, can recover the deterministic dynamics of the underlying continuous state space. The dynamics of such a model are a blend of the dynamics predicted by the deterministic continuous-state model and the cyclic dynamics predicted by the deterministic discrete-state model (Henson *et al*. 2001; Henson *et al*. 2003, King *et al.* 2002, King *et al.* 2004).

As it turns out, lattice effects are not theoretical oddities arising from simple population models. We were able to verify the existence of lattice effects in the chaotic treatments of the "hunt for chaos" experiment described earlier in this chapter (Henson *et al*. 2001). We present one example in detail.

Figure 12A shows a chaotic attractor of the LPA model. The data from the experimental treatment corresponding to this attractor clearly exhibit the temporal and phase space patterns of the predicted chaotic dynamics (King *et al*. 2004). However, the data also reveal a near 6-cycle pattern not predicted by the LPA model. We show that this unexpected 6-pattern is in fact a lattice effect.

Suppose that, in order to simulate dynamics on a whole integer lattice, we integerize the LPA model as follows. Since we manipulated the experimental parameters μ_a and c_{pa} by adding or subtracting integer numbers of adults, we can more accurately describe the experimental protocol by replacing the A-equation in the LPA model by an A-equation in which recruitment and survival are integer quantities. In addition, the survival/recruitment processes for the other state variables are fundamentally integer

processes. One possible deterministic lattice model for the experiment in question, and the one used in Henson *et al*. (2001) is

$$\begin{aligned} L_{t+1} &= \text{int}\left[bA_t \exp\left(-\frac{c_{ea}}{V} A_t - \frac{c_{el}}{V} L_t \right) \right], \\ P_{t+1} &= \text{int}\left[\left(1-\mu_l\right) L_t \right], \\ A_{t+1} &= \text{int}\left[P_t \exp\left(-\frac{c_{pa}}{V} A_t \right) \right] + \text{int}\left[\left(1-\mu_a\right) A_t \right]. \end{aligned} \tag{4}$$

This is a discrete state (or "lattice") LPA model. When $V = 1$, the lattice model predicts a 6-cycle attractor (Fig. 12B).

One stochastic version of the integerized LPA model results from adding demographic variability on the square root scale to the two unmanipulated life stage equations, namely to the equations for the larval and pupal stages:

$$\begin{aligned} L_{t+1} &= \text{int}\left[\left(\sqrt{bA_t \exp\left(-\frac{c_{ea}}{V} A_t - \frac{c_{el}}{V} L_t \right)} + E_{1t} \right)^2 \right], \\ P_{t+1} &= \text{int}\left[\left(\sqrt{\left(1-\mu_l\right) L_t} + E_{2t} \right)^2 \right], \\ A_{t+1} &= \text{int}\left[P_t \exp\left(-\frac{c_{pa}}{V} A_t \right) \right] + \text{int}\left[\left(1-\mu_a\right) A_t \right], \end{aligned} \tag{5}$$

where E_{1t} and E_{2t} are random normal variables with mean zero and variance-covariance matrix $\boldsymbol{\Sigma}$. In the rare cases in which a large negative E causes a negative value inside a square, we set the right hand side of that equation equal to zero. Equation (5) is a stochastic discrete state LPA model.

When $V = 1$, time series generated by the stochastic lattice model resembles the chaotic attractor; however, the lattice effect 6-pattern episodically recurs. See Fig. 12C.

The 6-pattern forecast by the stochastic lattice model is clearly evident in the three experimental replicates. Figure 13A shows the larval time series data from one replicate. The intermittently occurring 6-pattern is also seen in the phase space representation of the data (Fig. 13B).

Lattice effects can dramatically alter the predictions of ecological models, especially in systems for which the continuous-state deterministic dynamics are complex. In deterministic models, discretizing state space can replace a complicated continuous-state attractor with a simpler lattice attractor. Yet the continuous-state dynamics remain important inasmuch as they continue to shape the transient behavior on the lattice. In the presence of demographic variability, the system is influenced by both transients and attractors, and thus displays episodes which alternately resemble the dynamics of the continuous-state and lattice models. We emphasize that such lattice effects are not only found in relatively coarse lattices or in small populations: indeed, in our experimental study of chaotic population dynamics, lattice effects were important even with 10^7 lattice points.

ANATOMY OF CHAOS

Chaos is a mathematical concept. In reality, populations are stochastic, discrete-state systems. In the previous section we saw that, although discrete-state deterministic systems cannot exhibit chaos, discrete-state stochastic systems can exhibit a dynamic blend of lattice effects and what appears to be chaos. But can the chaotic signal be

quantified? What, in fact, do we mean when we say a discrete-state stochastic system is "chaotic"?

At the heart of chaos is the concept of sensitivity to initial conditions: a small perturbation can have a big effect. In populations, stochastic perturbations are not necessarily small, and they occur often. It is tempting to conclude that all fine structure associated with a chaotic mathematical model would be washed out by noise in experimental data. This is not necessarily the case.

Mathematically speaking, chaotic attractors are composed of infinitely many periodic orbits of saddle stability-type. Thus, chaotic dynamics exhibit continual fly-bys—not of saddle nodes as discussed in a previous section—but of saddle cycles. In time series, these fly-bys appear as recurrent episodes of near-periodic dynamics. Sensitivity to initial conditions rearranges the recurrent episodes but does not destroy them. Scientists studying oscillatory chemical reactions, electroencephalographic recordings, and epidemiological case-reports have all noted the appearance of recurrent near-periodic episodes in putatively chaotic dynamical systems (Lathrop and Kostelich, 1989; Schaffer *et al*. 1993; So *et al*. 1996, 1997).

Identification of cyclic episodes in time series requires a lot of data. For the oscillatory chemical reactions and electroencephalographic recordings mentioned above, it was possible to resolve these fine structures clearly because of the wealth of data. In the epidemiological study, however, the identification of these patterns was confined to cycles of periods one and two, even though the data set afforded by measles case-reports in major cities are extensive by ecological standards (Schaffer *et al*. 1993). There is, in fact, a dearth of long ecological time series. The 8-year long *Tribolium* data set

(≈ 70 generations) from the "hunt for chaos" experiment represents a unique opportunity to examine the signal of chaos as it is manifest in biological populations.

We have developed the following hypothesis. Populations, being discrete-state stochastic systems, should display episodes of lattice cycles interspersed with episodes of chaotic signal. The chaotic signal itself should exhibit recurrent episodes of cyclic behavior. Chaotic population time series therefore should be a mixture of cycles predicted by both the discrete-state and continuous-state models, woven together by stochasticity. In this section we present a tool to test this hypothesis.

For the chaotic ($c_{pa} = 0.35$) treatment in the "hunt for chaos" experiment there are a large number of model-predicted periodic orbits. They are of two types: (1) saddle-cycles embedded in the continuous-state LPA model attractor and (2) lattice cycles of the discrete-state LPA model. Although there are infinitely many of the first type, the level of demographic variability and the length of the data time-series puts a limit on our ability to distinguish among these cycles. Thus we focus our attention on a dominant period-11 saddle-cycle. At the same parameter estimates, the discrete-state LPA model has precisely nine periodic orbits. These orbits fall into three groups based on their periodicity: 3-cycles, 6-cycles, and 8-cycles. Cycles within each of the groups are very similar, with none differing from any other by more than 30 animals. Figure 14 shows the period-11 saddle-cycle and the lattice 3, 6, and 8-cycles.

We can quantify fly-bys of periodic orbits using a measure of the "distance" between data points and periodic orbits. We generalize the notion of distance using a quantity we call the *lag-metric comparison*, or LMC. Essentially, the LMC measures the average distance in state space between the data and each phase of the model cycle. To be

precise, given a length-N sequence of data vectors, $d = \{d_t\}_{t=0}^{N-1}$ and a model of period-T cycle, $\{m_t\}_{t=0}^{\infty}\ (m_{t+T} = m_t)$ we define the LMC of d and m at lag s and time t by the formula

$$LMC(s,t) = \frac{1}{T}\sum_{q=0}^{T-1}\left\|d_t - m_{t+s-q}\right\|,$$
$$s = 0,...,T-1, \quad t = T-1,...,N-1,$$

where $\|x\| = |x_1| + |x_2| + |x_3|$ is a norm on the three-dimensional state space. In Figure 15, we plot $LMC(s,t)$ against t directly.

Figure 15 shows plots of the LMC of the data from replicate 13 of the "hunt for chaos" experiment against time. At any time t a low value of the LMC indicates that the data lie close to the model-predicted T-cycle and have done so over the course of the preceding T time units; a high LMC value indicates poor correspondence between model cycle and data. Plotted against time, the LMC appears as a "braid" with one strand for each phase. Time intervals over which the data trajectory closely follows the model cycle ("cycle episodes" for short) appear as unplaited portions of the braid. Tightly plaited portions indicate lack of correspondence between data and the particular model cycle in question.

Viewing the complete 424-week replicate 13 data series using the LMC, we see that, initially, the population trajectory follows the saddle 11-cycle. During this same interval, the lattice 8-cycle is also evident. This is not surprising, since these two cycles lie close together. After about week 50, a 6-cycle episode is identified. Over weeks 110-134, another 8-cycle/11-cycle episode appears, which is followed by a 3-cycle episode

over weeks 150-172. At around week 200, a 130-week 6-cycle episode begins. Weeks 328-356 display another 11-cycle/8-cycle episode. Finally, it should be noted that a 1-cycle episode (i.e., an equilibrium fly-by) is evident in these data around week 364.

Overall, the pattern we observe in the data is one of transient but recurrent near-periodic episodes, each traceable to a model-predicted periodic orbit. From this perspective, the principal role of stochasticity is to move the system from one cycle to another. The set of patterns observed, as well as their relative prominence in the mixture, is a prediction of the mathematical model. It is worth pointing out that this method of quantifying the influence of chaos in population data is based on the fine structure of the dynamics. By contrast, commonly-used measures, such as the "stochastic Liapunov exponent" are long-time averages which can measure only the gross properties of an entire system.

MECHANISTIC MODELS OF THE STOCHASTICITY

We have presented three stochastic LPA models in this chapter: the lognormal model (2), the square root model (3), and the integerized square root model (5). Although these models have been useful, stochasticity was introduced to the deterministic skeleton through the addition of biologically unspecified random variables. A next step is to associate more carefully the uncertainty to biological features such as reproduction and survival.

A simple stochastic model of this type for the population dynamics of the beetle uses the binomial and Poisson distributions to characterize the aggregation of

demographic events within the life stages (Dennis *et al*. 2001, Henson *et al.* 2003, Desharnais *et al*. 2004). The Poisson-binomial (PB) model is

$$
\begin{aligned}
L_{t+1} &\sim Poisson\left[ba_t \exp\left(-\frac{c_{ea}}{V} a_t - \frac{c_{el}}{V} l_t \right) \right] \\
P_{t+1} &\sim Binomial\left[l_t, (1-\mu_l) \right] \\
R_{t+1} &\sim Binomial\left[p_t, \exp\left(-\frac{c_{pa}}{V} a_t \right) \right] \\
S_{t+1} &\sim Binomial\left[a_t, (1-\mu_a) \right] \\
A_{t+1} &= R_{t+1} + S_{t+1}
\end{aligned}
\tag{6}
$$

where L_{t+1} is the number of feeding larvae, P_{t+1} is the number of non-feeding larvae, pupae, and callow adults, R_{t+1} is the number of sexually mature adult recruits, S_{t+1} is the number of surviving mature adults, and l_t, p_t, r_t, and s_t are the respective abundances observed at time t. The total number of mature adults A_{t+1} is given by $R_{t+1} + S_{t+1}$, and $a_t = r_t + s_t$ is the total number of mature adults observed at time t. Here "~" means "is distributed as."

The PB model (6) has purely demographic variability. The L-stage is a compound process: a random number of potential recruits are produced with conditional mean ba_t, and each potential recruit subsequently undergoes a survival process in which the conditional survival probability $\exp(-c_{el} l_t - c_{ea} a_t)$ depends on the system state variables l_t and a_t. We assume that the number of potential recruits has a Poisson ba_t distribution, and that the number of subsequent survivors has a binomial distribution. The conditional

distribution of L_{t+1} given $L_t = l_t$ and $A_t = a_t$ becomes a Poisson distribution with mean $ba_t \exp(-c_{el} l_t - c_{ea} a_t)$.

The distribution of P_{t+1} given $L_t = l_t$ has a binomial $(l_t, (1-\mu_l))$ distribution. The A-stage equation is the sum of two survival processes: recruits from the P-stage, denoted R_{t+1}, and surviving adults, denoted S_{t+1}. We assume that R_{t+1} given $P_t = p_t$ and $A_t = a_t$ has a binomial $(p_t, \exp(-c_{pa} a_t))$ distribution. The P-stage survival probability is the nonlinear function $\exp(-c_{pa} a_t)$. S_{t+1} is assumed to have a binomial $(a_t, (1-\mu_a))$ distribution.

In the PB model there are no noise variances and covariances to be estimated. The stochastic model has the same number of parameters as the deterministic LPA model (1). State space is discrete. The PB model is a stochastic lattice (integer valued) model. The assumption of demographic variability seems appropriate for laboratory cultures of beetles grown under standard conditions. We have used this type of model to study competition between two species of flour beetle where competitive exclusion is a common outcome (Desharnais *et al*. 2004).

BEYOND BEETLES

The rarity of designed manipulations and replications in natural systems makes rigorous testing of models difficult. Models of natural systems must necessarily be evaluated on the basis of biological plausibility, how well they describe the data, and, when possible, how well they predict new data. Models of natural systems retain the status of hypotheses and are used only tentatively as building blocks in theories about population abundance

patterns. Our laboratory documentation of nonlinear phenomena such as saddles nodes, phase switching, bifurcations, lattice effects, and chaos suggests that these phenomena may be worthy hypotheses to incorporate into investigations by field ecologists.

What are the prospects for finding this sort of fine-structure in the dynamics of natural systems? Clearly, we have exploited some special features of the *Tribolium* system. Foremost among these are: a very detailed understanding of the life history and population biology of the organism, the ability to observe all essential state variables, the absence of measurement error, the ability to essentially eliminate environmental variability, and the isolation of each population from interaction with other populations. In systems with different properties, the attainable resolution may be coarser. We hope our research using the *Tribolium* model system, however, will raise expectations for how quantitatively precise the model/data fit can be in population biology.

Ecologists can be encouraged that simple nonlinear models can help unlock substantial gains in understanding population systems. Keys to transforming nonlinear models from scientific caricatures to testable scientific hypotheses are: incorporating demographic/environmental variability as well as the deterministic signal in biologically based models, explicitly connecting models and data, including statistics in the mathematical analysis, rigorously evaluating model performance, and effectively combining biology, mathematics, and statistics in an interdisciplinary approach.

Our use of a laboratory population system served the purpose that laboratory experiments have always served: to isolate factors and to rigorously attribute cause. We were interested in whether the concepts from nonlinear dynamics—cycles, multiple attractors, chaos—could ever advance beyond the status of hypotheses and be convincing

explanations of population fluctuations. We were interested in whether a mathematical population model could ever be considered reliable scientific knowledge. The laboratory allowed us to manipulate conditions, perform a census of each population, and replicate, so that key predictions of the model could be tested.

Our results strengthen the relevance of mathematical modeling in population ecology. Not only was a mathematical model *useful* in describing population patterns, it was *essential* for understanding the experimental results. Nonlinear dynamical concepts, combined with stochasticity, *are* the explanations of the phenomena that we documented. In addition, advanced statistical modeling techniques were *required* for connecting model and data. Throughout much of ecology, mathematical models have been no more than simplified teaching concepts, not to be taken seriously, and statistics has been a set of recipes for data analysis. Herein we have displayed a population system in which mathematical modeling and mathematical statistics form an integral part of the theories themselves.

REFERENCES

Bailey, B. A., Ellner, S., and Nychka, D. W. 1997. Chaos with confidence: asymptotics and applications of local Lyapunov exponents. In: *Nonlinear Dynamics and Time Series: Building a Bridge Between the Natural and Statistical Sciences* (eds. Cutler, C. and Kaplan, D. T.) American Mathematical Society, Providence, RI.

Costantino, R. F., Cushing, J. M., Dennis, B., and Desharnais, R. A. 1995. Experimentally induced transitions in the dynamic behavior of insect populations. *Nature* **375**: 227–230.

Costantino, R. F., Desharnais, R. A., Cushing, J. M., and Dennis, B. 1997. Chaotic dynamics in an insect population. *Science* **275**: 389–391.

Costantino, R. F. and Desharnais, R. A. 1991. *Population dynamics and the Tribolium model: genetics and demography*. Springer-Verlag, New York, New York, USA.

Cushing, J. M., Dennis, B., Desharnais, R. A., and Costantino, R. F. 1998. Moving toward an unstable equilibrium: saddle nodes in population systems. *Journal of Animal Ecology* **67**: 298-306.

Cushing, J. M., Henson, S. M., Desharnais, R. A., Dennis, B., Costantino, R. F., and King, A. A. 2001. A chaotic attractor in ecology: theory and experimental data. *Chaos, Solitons and Fractals* **12**: 219–234.

Cushing, J. M., Costantino, R. F., Dennis, B., Desharnais, R. A., and Henson, S. M. 2003. *Chaos in Ecology: A Study of Nonlinear Systems.* Academic Press, New York.

Dennis, B. 2002. Allee effects in stochastic populations. *Oikos* **96**: 389-401.

Dennis, B., Desharnais, R. A., Cushing, J. M., and Costantino, R. F. 1995. Nonlinear demographic dynamics: Mathematical models, statistical methods, and biological experiments. *Ecological Monographs* **65**: 261–281.

Dennis, B., Desharnais, R. A., Cushing, J. M., and Costantino, R. F. 1997. Transitions in population dynamics: Equilibria to periodic cycles to aperiodic cycles. *Journal of Animal Ecology* **66**: 704–729.

Dennis, B., Desharnais, R. A., Cushing, J. M., Henson, S. M., and Costantino, R. F. 2001. Estimating chaos and complex dynamics in an insect population. *Ecological Monographs* **71**: 277–303.

Dennis, B., Desharnais, R. A., Cushing, J. M., Henson, S. M., and Costantino, R. F. 2003. Can noise induce chaos? *Oikos* **102**: 329–340.

Desharnais, R. A., and Costantino, R. F. 1980. Genetic analysis of a population of *Tribolium*. VII. Stability: Response to genetic and demographic perturbations. *Canadian Journal of Genetics and Cytology* **22**: 577–589.

Desharnais, R. A., Costantino, R. F., Cushing, J. M., and Dennis, B. 1997. Estimating chaos in an insect population. *Science* **276**: 1881–1882.

Desharnais, R. A., Costantino, R. F., Cushing, J. M., Henson, S. M., and Dennis, B. 2001. Chaos and population of insect outbreaks. *Ecology Letters* **4**: 229–235.

Desharnais, R. A., Edmunds, J., Costantino, R. F., and Henson, S. H. 2004. Species competition: Uncertainty on a double invariant loop. *Journal of Difference Equations and Applications* (in press).

Doebeli, M. 1993. The evolutionary advantage of controlled chaos. *Proceedings of the Royal Society London B*. **254**: 281-285.

Domokos, G. and Scheuring, I. 2002. Random perturbations and lattice effects in population dynamics. *Science* **297**: 2163.

Ellner, S. and Turchin, P. 1995. Chaos in a noisy world: new methods and evidence from time-series analyses. *The American Naturalist* **145**: 343-375.

Hastings, A., Holm, C. L., Ellner, S., Turchin, P., and H. C. J. Godfray. 1993. Chaos in ecology: Is mother nature a strange attractor? *Annual Review of Ecology and Systematics* **24**: 1-33.

Hawkins, B. A., and Cornell, H. V. 1999. *Theoretical Approaches to Biological Control*. Cambridge University Press, New York.

Henson, S. M., Cushing, J. M., Costantino, R. F., Dennis, B., and Desharnais, R. A. 1998. Phase switching in population cycles. *Proceedings of the Royal Society*, *London B* **265**: 2229–2234.

Henson, S. M., Costantino, R. F., Cushing, J. M., Desharnais, R. A., and King, A. A. 2001. Lattice effects observed in chaotic dynamics of experimental populations. *Science* **294**: 602–605.

Henson, S. M., King, A. A., Costantino, R. F., Cushing, J. M., Dennis, B., and Desharnais, R. A. 2003. Explaining and predicting patterns in stochastic population systems. *Proceedings of the Royal Society of London B* **270**: 1549-1553.

Jackson, E. A. 1989. *Perspectives of Nonlinear Dynamics*, Cambridge University Press, Cambridge, vol. 1, pp. 216-219.

Kendall, B. E., Briggs, C. J., Murdock, W. W., Turchin, P., Ellner, S. P., McCauley, E., Nisbet, R. M., and Wood, S. N. 1999. Why do populations cycle? A synthesis of statistical and mechanistic modeling approaches. *Ecology* **80**: 1789-1805.

Kendall, B. E., Schaffer, W. M., Olsen, L. F., Tidd, C. W., and Jorgensen, B. L. 1993. in *Predictability and Nonlinear Modelling in Natural Sciences and Economics*, eds. Grassman, J. and van Straten, G., Kluwer, Dordrecht, The Netherlands, pp. 184-203.

King, A. A., Desharnais, R. A., Henson, S. M., Costantino, R. F., and Cushing, J. M. 2002. Random perturbations and lattice effects in chaotic population dynamics. *Science* **297**:2163.

King, A. A., Costantino, R. F., Cushing, J. M., Henson, S. M., Desharnais, R. A., and Dennis, B. 2004. Anatomy of a chaotic attractor: Subtle model-predicted patterns revealed in population data. *Proceedings of the National Academy of Science* (USA) **101**: 408-413.

Klimko, L. A. and Nelson, P. I. 1978. On conditional least squares estimation for stochastic processes. *Annals of Statistics* **6**: 629-642.

Lathrop, D. P. and Kostelich, E. J. 1989. Characterization of an experimental strange attractor by periodic orbits. *Physical Review A* **40**: 4028-4031.

May, R. M. 1974. Biological populations with nonoverlapping generations: stable points, stable cycles, and chaos. *Science* **186**: 645-647.

Mertz, D. B. 1972. The *Tribolium* model and the mathematics of population growth. *Annual Review of Ecology and Systematics* **3** : 51-78.

Olsson, D. M. and Nelson, L. S. 1975. The Nelder-Mead simplex procedure for function minimization. *Technometrics* **17**: 45-51.

Park, T. 1955. Experimental competition in beetles, with some general implications. In: *The Numbers of Man and Animals*, Craig, J. B. and Pirie, N. W. eds. 69-82, Oliver & Boyd, London.

Perry, J. N., Smith, R. H., Woiwod, I. P., and Morse, D. R., eds. 2000. *Chaos in Real Data: The Analysis of Nonlinear Dynamics from Short Ecological Time Series*, Kluwer, Dordrecht, The Netherlands.

Press, W. H., Flannery, B. P., Teukolsky, S. A., and Vetterling, W. T. 1986. *Numerical recipes: the art of scientific computing.* Cambridge University Press, Cambridge, England.

Schaffer, W. M., Kendall, B. E., Tidd, C. W., and Olson, L. F. 1993. Transient periodicity and episodic predictability in biological dynamics. *IMA Journal of Mathematics Applied in Medicine and Biology* **10**: 227-247.

Shaffer, M. L. 1981. Minimum population sizes for species conservation. *BioSciences* **31**: 131-134.

Shulenburger, L., Ying-Cheng, L., Yalcinkaya, T. and Holt, R. D. 1999. Controlling transient chaos to prevent species extinction. *Physics Letters* **66**: 1123-1125.

Simberloff, D. 1988. The contribution pf population and community ecology to conservation science. *Annual Review of Ecology and Systematics* **19**: 473-511.

So, P., Ott, E., Schiff, S. J., Kaplan, D. T., Sauer, T. and Grebogi, C. 1996. Detecting unstable periodic orbits in chaotic experimental data. *Physical Rev*iew *Letters* **76**: 4705-4708.

So, P., Ott, E. Sauer, Gluckman, B. J., Grebogi, C. and Schiff, S. J. 1997. Extracting unstable periodic orbits from chaotic time series data. *Physical Review E* **55**: 5398-5417.

Sole, R. V., Gamarra, J. G. P., Ginovart, M., and Lopez, D. 1999. Controlling chaos in ecology: from deterministic to individual based models. *Bulletin of Mathematical Biology* **61**: 1187-1207.

Stuart, A., and Ord, J. K. 1991. *Kendall's advanced theory of statistics*. Volume 2: classical inference and relationships. Fifth edition. Griffin, London, England.

Tong, H. 1990. *Nonlinear time series: a dynamical system approach*. Oxford University Press, Oxford, England.

Turchin, P. 2003. *Complex Population Dynamics: A Theoretical/Empirical Synthesis*. Princeton University Press, Princeton, New Jersey.

Turchin, P., and Ellner, S. P. 2000. Living on the edge of chaos: population dynamics of Fennoscandian voles. *Ecology* **81**: 3099–3116.

Wilson, E. O. 2002. *The Future of Life*, Alfred Knopf, New York.

Wilson, H. B. and Hassell, M. P. 1993. Detecting chaos in noisy time series. *Proceedings of the Royal Society of London, B* **253**: 239-244.

Xu, D., Li, Z., Bishop, S. R., and Galvanetto, U. 2002. Estimation of periodic-like motions of chaotic evolutions using detected unstable periodic patterns. *Pattern Recognition Letters* **23**: 245-252.

Zimmer, C. 1999. Life after chaos. *Science* **284**: 83-86.

ACKNOWLEDGEMENTS

This research was supported, in part, by National Science Foundation grants DMS-9625576, DMS-9616205, DMS-9981374, DMS-9973126, DMS-9981458, DMS-9981423, DMS-0210474, DMS-0414212.

FIGURE CAPTIONS

Fig. 1. Time series data (closed circles) and one-step forecasts (open circles) for the control replicate A from the experiment of Desharnais and Costantino (1980). Solid lines connect the observed census data. Dashed lines connect the observed numbers at time t with the one-step forecast at time t+1. The maximum likelihood parameter estimates are $b = 11.67, c_{el} = 0.0093, c_{ea} = 0.0110, c_{pa} = 0.0178, \mu_l = 0.5129, \mu_a = 0.1108$.

Fig. 2. Bifurcation diagram for the LPA model (1) with adult mortality μ_a as the bifurcation parameter. The maximum likelihood parameter estimates are $b = 7.48, c_{ea} = 0.0091, c_{pa} = 0.0041, c_{el} = 0.0120, \mu_l = 0.2670$. The arrows indicate those values of μ_a at which experiments were conducted.

Fig. 3. Phase space plots of the data (SS genetic strain) obtained from the bifurcation experiment with $\mu_a = 0.04$ (equilibrium), $\mu_a = 0.27, 0.50$ (2-cycles), $\mu_a = 0.73$ (equilibrium) and $\mu_a = 0.96$ (invariant loop).

Fig. 4. Bifurcation diagram for the LPA model (1) using c_{pa} as the bifurcation parameter. The adult death rate was set experimentally at $\mu_a = 0.96$. The other parameter values are $b = 10.45, \mu_l = 0.2000, c_{el} = 0.01731, c_{ea} = 0.01310$. The arrows indicate those c_{pa} values at which experiments were performed.

Fig. 5. Phase-space plots for the data and stochastic model (3) of the experiment associated with the bifurcation diagram in Fig. 4. The model simulations used $\mu_a = 0.007629$ for the controls, $\mu_a = 0.96$ for the treatments where adult mortality was manipulated, and the c_{pa} value given in the figure together with the conditional least squares parameter estimates $b = 10.45$, $c_{el} = 0.01731$, $c_{ea} = 0.01310$, $\mu_l = 0.2000$ and the following variance-covariance estimates: $\hat{\sigma}_{11} = 1.621$, $\hat{\sigma}_{12} = -0.1336$,

$\hat{\sigma}_{13} = -0.01339$, $\hat{\sigma}_{22} = 0.7375$, $\hat{\sigma}_{23} = -0.0009612$, and $\hat{\sigma}_{33} = 0.01212$ for the controls and $\hat{\sigma}_{11} = 2.332$, $\hat{\sigma}_{12} = 0.007097$, $\hat{\sigma}_{22} = 0.2374$, and $\hat{\sigma}_{13} = \hat{\sigma}_{23} = \hat{\sigma}_{33} = 0$ for the treatments where adult mortality and recruitment were manipulated.

Fig. 6. Chaotic attractor of the deterministic LPA model in phase space. The pictures were generated from 2000 iterations of the LPA model after the initial transients disappeared. The attractor is shaded according to λ_t, the logarithm of largest moduli of the three eigenvalues of the Jacobian matrix of the LPA model (1) evaluated at the point (L_t, P_t, A_t) using $\mu_a = 0.96$, $c_{pa} = 0.35$, and the conditional least squares parameter estimates listed in the caption of figure 5. The colors range from light gray for negative values ($\lambda_t < 0$), to dark gray for moderate values ($0 \leq \lambda_t \leq 3$), to black for large positive values ($\lambda_t > 3$). (A) The full attractor has "hot regions" (black) where the trajectories show strong divergence and "cold regions" (light gray) where trajectories converge. (B) The axis scale for adult numbers is changed to magnify the base of the attractor. The grids show the boundary of the "in-box" and "out-box" regions used in the experimental design described in the text. The "hot spots" of the attractor fall mostly within this box.

Fig. 7. Time series of larval numbers for the stochastic model and experimental data under three conditions: unperturbed treatment, in-box treatment, and out-box treatment. The simulations are from the demographic stochastic model (3) with $\mu_a = 0.96$, $c_{pa} = 0.35$, and the conditional least squares parameter and variance-covariance estimates listed in the caption of figure 5.

Fig. 8. The time series of larval (circles), pupal (triangles), and adult (squares) numbers. (A) Deterministic model which reveals no influence of the presence of the unstable equilibrium. (B) Stochastic model (3) with a saddle fly-by displayed in the interval marked by the double ended arrow. (C) Experimental data with a saddle fly-by seen in the interval from $t = 8$ to $t = 17$. The deterministic and stochastic model simulations used $\mu_a = 0.96$, $c_{pa} = 0.05$, and the conditional least squares parameter estimates listed in the caption of figure 5. The stochastic model also used the and variance-covariance estimates listed in the caption of figure 5.

Fig. 9. The model predicted invariant loop (closed curve) and unstable equilibrium (closed circle) for the hunt experiment treatment $c_{pa} = 0.05$ are shown together (in phase-space) with the data orbit of one replicate (open circles). Lines connect the data values through time.

Fig. 10. Time series data showing phase switching in population cycles. (A) Replicate A (circles) changes phase at time step 4 while replicate B (triangles) changes phase at time step 4 and 14. After time step 14 both replicates from the experiment of Desharnais and Costantino (1980) are asynchronous. (B) Replicate 4 (circles) does not change phase. Replicate 22 (triangles) changes phase at time step 10. After time step 10 both replicates from the experiment of Costantino *et al*. (1995) are asynchronous. (C) Replicates 3, 18, and 23 from the experiment of Costantino *et al*. (1997) show 3-cycle dynamics (transient time steps zero to four are omitted for clarity). Replicate 23 (squares) does not shift

phase. Replicate 3 (circles) changes phase at time step 8. Replicate 18 (triangles changes phase at time step 13 and at time step 18. After time step 18 all three replicates are out of phase.

Fig. 11. Model predictions and the data. Time series for the deterministic model (1) were generated for the L-stage using maximum likelihood parameter estimates $b = 11.67$, $\mu_l = 0.5129$, $c_{pa} = 0.0178$, $c_{ea} = 0.0110$, $c_{el} = 0.0093$, $\mu_a = 0.1108$ and the initial condition [70, 36, 64]. Time series for the stochastic model (2) were generated for the L-stage using the same parameter estimates and initial condition as for the deterministic model and the variance-covariance estimates $\hat{\sigma}_{11} = 0.2771$, $\hat{\sigma}_{12} = 0.02792$, $\hat{\sigma}_{13} = 0.009796$, $\hat{\sigma}_{22} = 0.4284$, $\hat{\sigma}_{23} = -0.008150$, and $\hat{\sigma}_{33} = 0.01112$. (A) The deterministic time series approaches a 2-cycle. (D) In composite phase space, the corresponding solution of the composite LPA map approaches the fixed point $[L, P, A]_\Delta$ = [18,158,106]. (B) The stochastic model L-stage time series, on the other hand, shifts phase at time t = 7 and again at t = 15. (E) In composite phase space, these phase changes occur exactly when the basin boundary is crossed. The data for replicate B from the experiment of Desharnais and Costantino (1980) are shown in panels (C) and (F). As the LPA model predicts, phase shifting occurs in the data time series precisely when the data cross the model predicted basin boundary in composite phase space.

Fig. 12. Density dynamics of the LPA models with b = 10.67, μ_l = 0.1955, μ_a = 0.96, c_{el} = 0.01647, c_{ea} = 0.01313, c_{pa} = 0.35. For the demographic stochastic model (3), the variance and covariance entries of the matrix Σ were taken to be σ_{11} = 2.332,

$\sigma_{22} = 0.2374$ and $\sigma_{12} = \sigma_{21} = 0$. (A) The chaotic attractor of LPA model (1). (B) A 6-cycle attractor of the lattice LPA model with $V = 1$ (on the order of 107 lattice points). (C) A stochastic realization with $V = 1$ exhibits a mixture of patterns, with intermittent patterns that resemble the lattice 6-cycle in panel (B) interspersed among episodes that resemble the chaotic attractor in panel (A).

Fig. 13. A 304 week data time series obtained from one replicate of the *Tribolium* experiment (Dennis *et al*. 2001) where adult mortality and recruitment were manipulated to be $\mu_a = 0.96$ and $c_{pa} = 0.35$. (A) Selected temporal episodes that resemble the lattice model 6-cycle shown in Fig. 12B are displayed as open circles. The remaining data points (closed circles) resemble the chaotic time series. (B) The selected temporal episodes in (A) are shown in phase space (on the order of 10^7 lattice points). Compare the 6-pattern episodes (open circles) to the 6-cycle lattice attractor in Fig. 12B.

Fig. 14. Model-predicted continuum and lattice cycles. The four small phase-space graphs depict the 11-cycle from the continuous-state model (1) and the 8-, 6-, 3-cycles from the discrete-state deterministic model (4). In the central graph, all the cycles are superimposed on the chaotic attractor of the deterministic model. The graphs were generated by using the conditional least-squares parameter estimates $b = 10.45, c_{ea} = 0.01310, c_{el} = 0.01731, \mu_a = 0.2000$ with $\mu_a = 0.96, c_{pa} = 0.35$ both set experimentally.

Fig. 15. Lag-metrics in the data. (A) Raw time-series data. For clarity, only the L-stage numbers are shown. LMC with respect to the model-predicted cycles: (B) continuous-state model saddle 11-cycle; (C) discrete-state model 8-cycle; (D) discrete-state model 6-cycle; and (E) discrete-state model 3-cycle. During intervals for which the "braid" appears tightly plaited, the data bear little or no resemblance to the corresponding model-predicted cycle. Unplaited portions of the braid correspond to intervals for which the data closely resemble the model cycle. As shown in panel (F), we identified T-cycle episodes by setting the threshold number of animals $\theta = 55$ (dashed line) and threshold duration $K = 12$ for all model-predicted cycles. Thus, to be identified as a T-cycle episode in panel (F), non-equilibrium patterns were required to be in evidence for 24 consecutive weeks (more than seven generations), a very stringent requirement. The effects of varying θ and/or K on the episodes identified can be readily seen from inspection of the LMC plots in panels B-E.

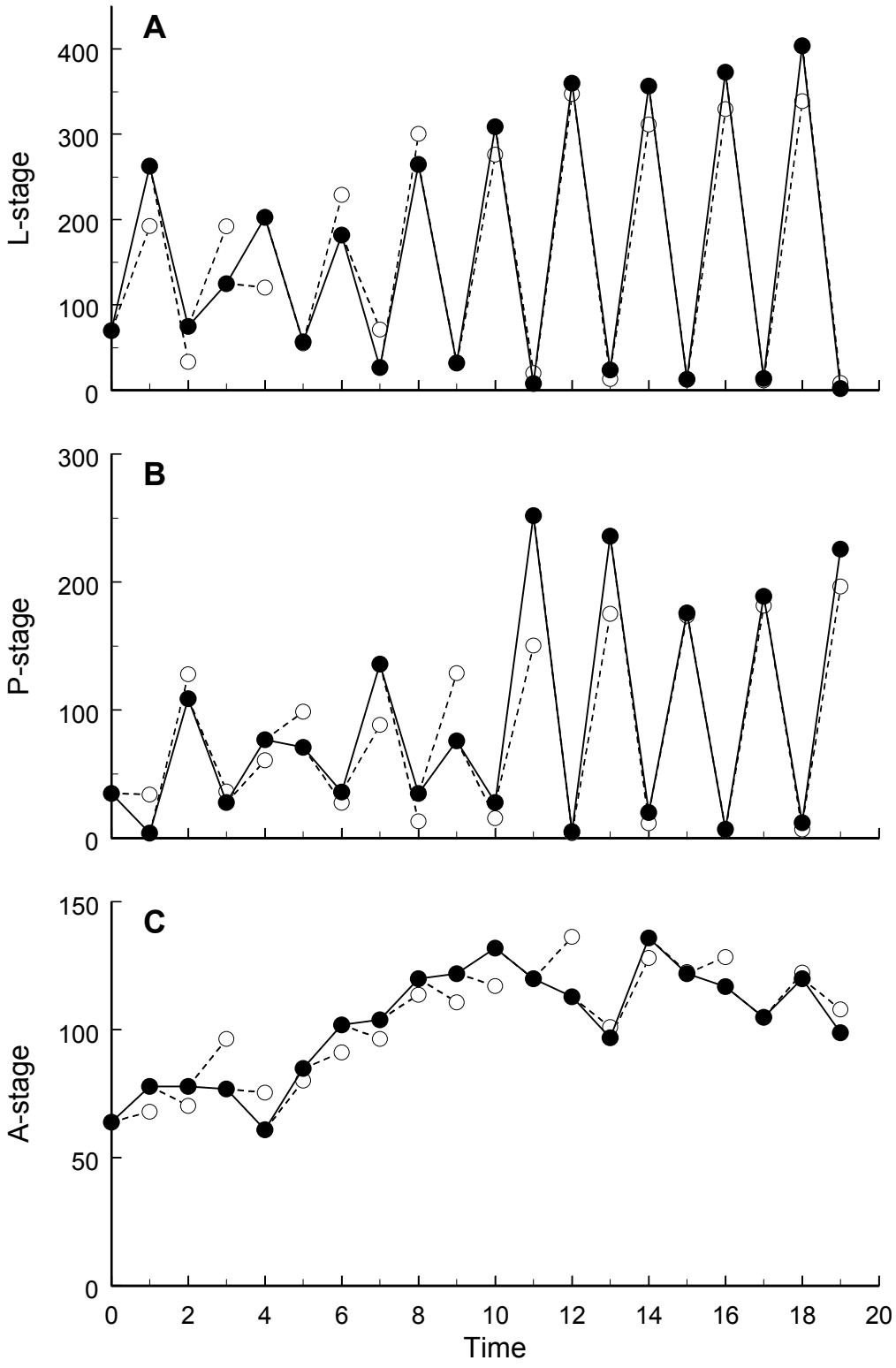
A
L-stage
400
300
200
100
0
B
P-stage
300
200
100
0
C
A-stage
150
100
50
0
0
2
4
6
8
10
12
14
16
18
20
Time

Figure 1

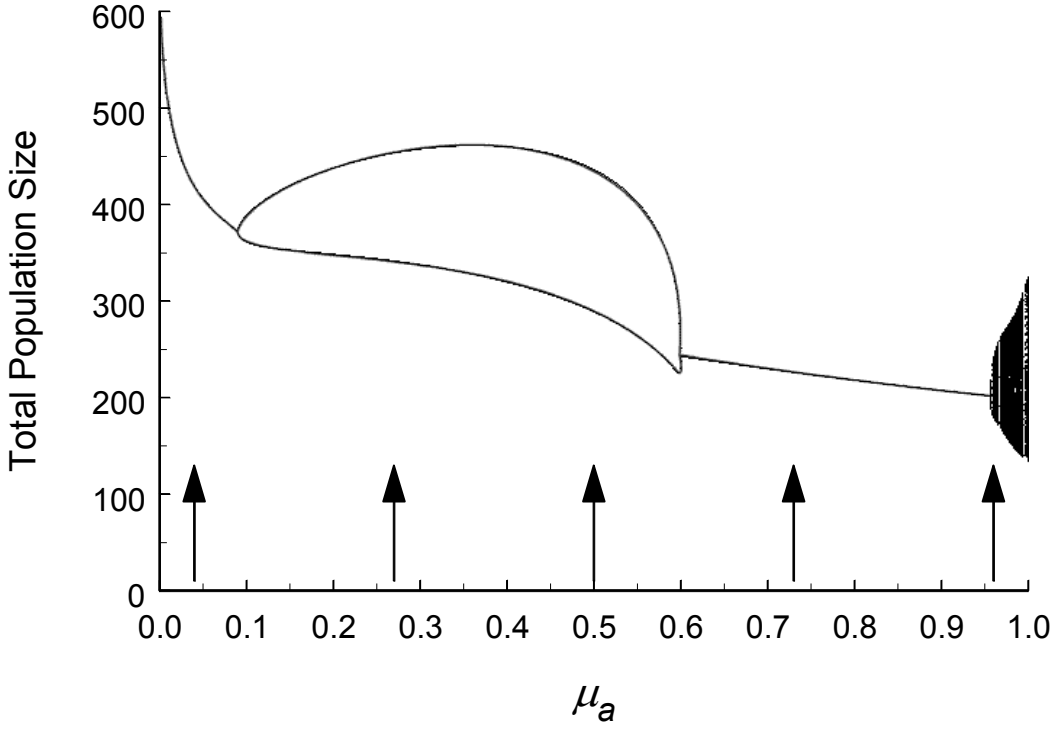
Total Population Size
600
500
400
300
200
100
0
0.0
0.1
0.2
0.3
0.4
0.5
0.6
0.7
0.8
0.9
1.0
μ_a

Figure 2

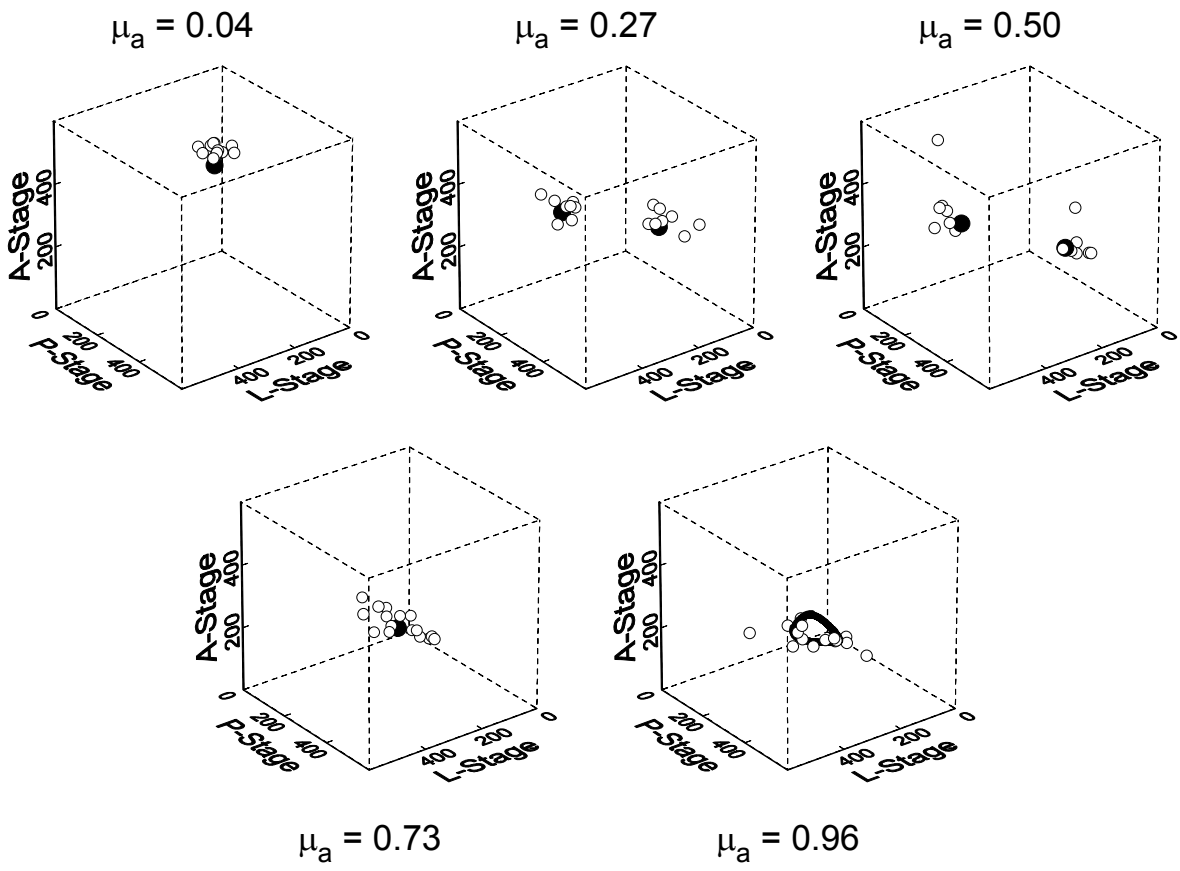
μ_a = 0.04
μ_a = 0.27
μ_a = 0.50
μ_a = 0.73
μ_a = 0.96
A-Stage
P-Stage
L-Stage
0
200
400

Figure 3

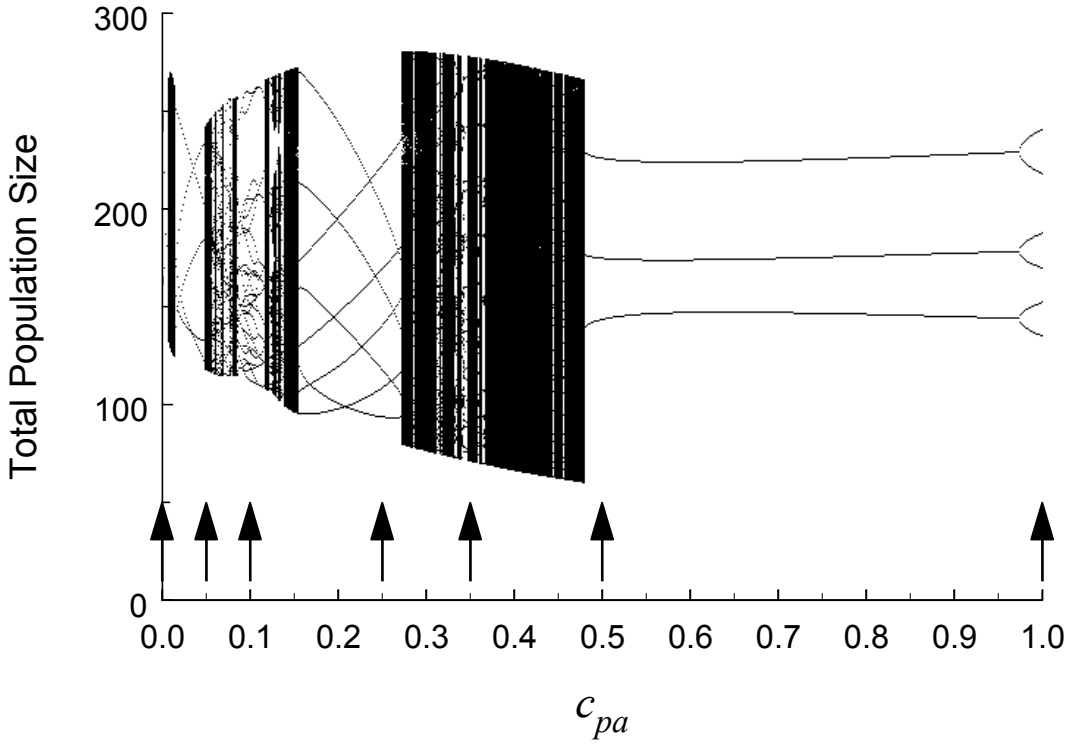
300
200
100
0
Total Population Size
0.0
0.1
0.2
0.3
0.4
0.5
0.6
0.7
0.8
0.9
1.0
c_{pa}

Figure 4

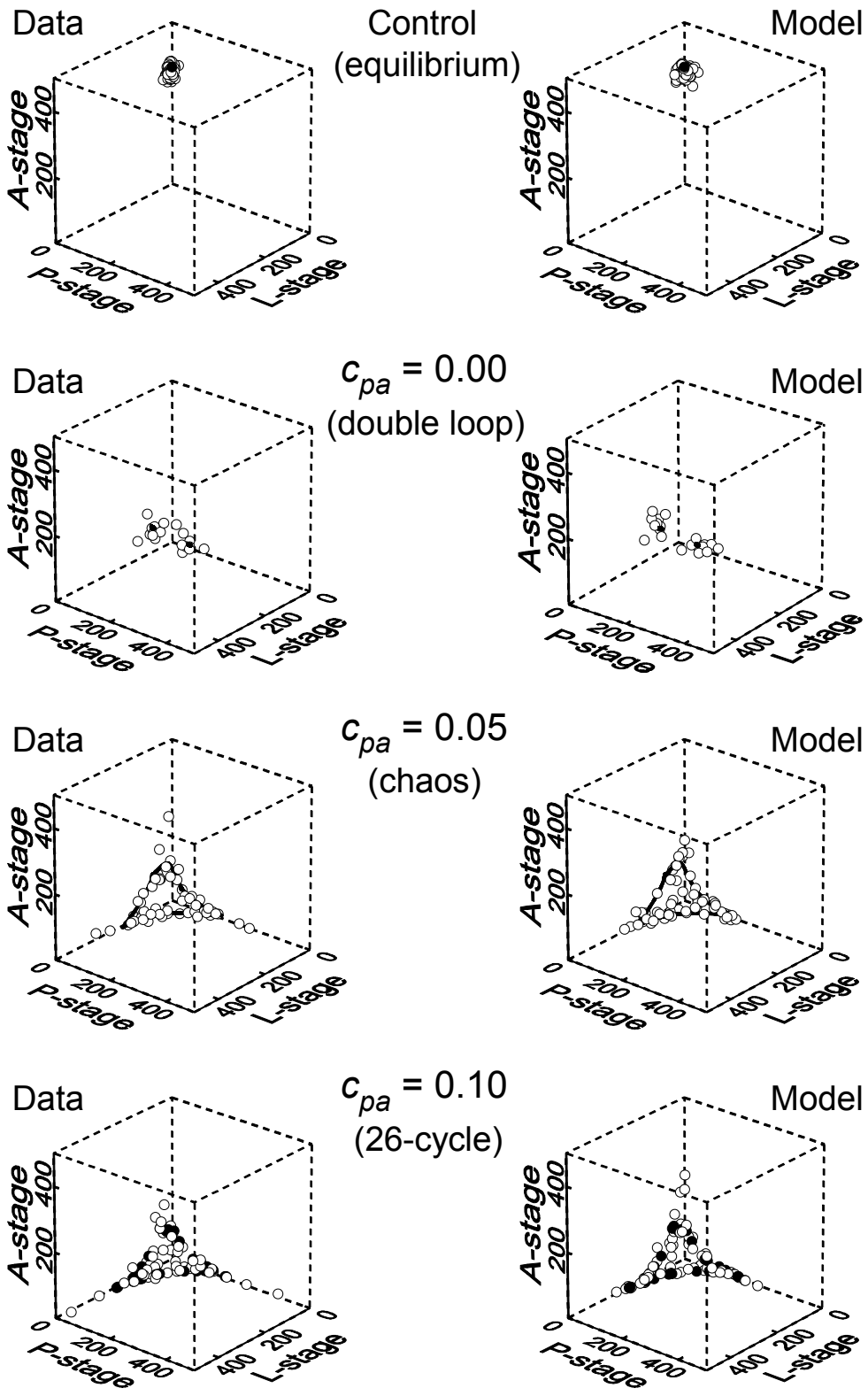
Data
Control
(equilibrium)
Model
A-stage
P-stage
L-stage
0
200
400
Data
c_{pa} = 0.00
(double loop)
Model
Data
c_{pa} = 0.05
(chaos)
Model
Data
c_{pa} = 0.10
(26-cycle)
Model

Figure 5 (pt. 1)

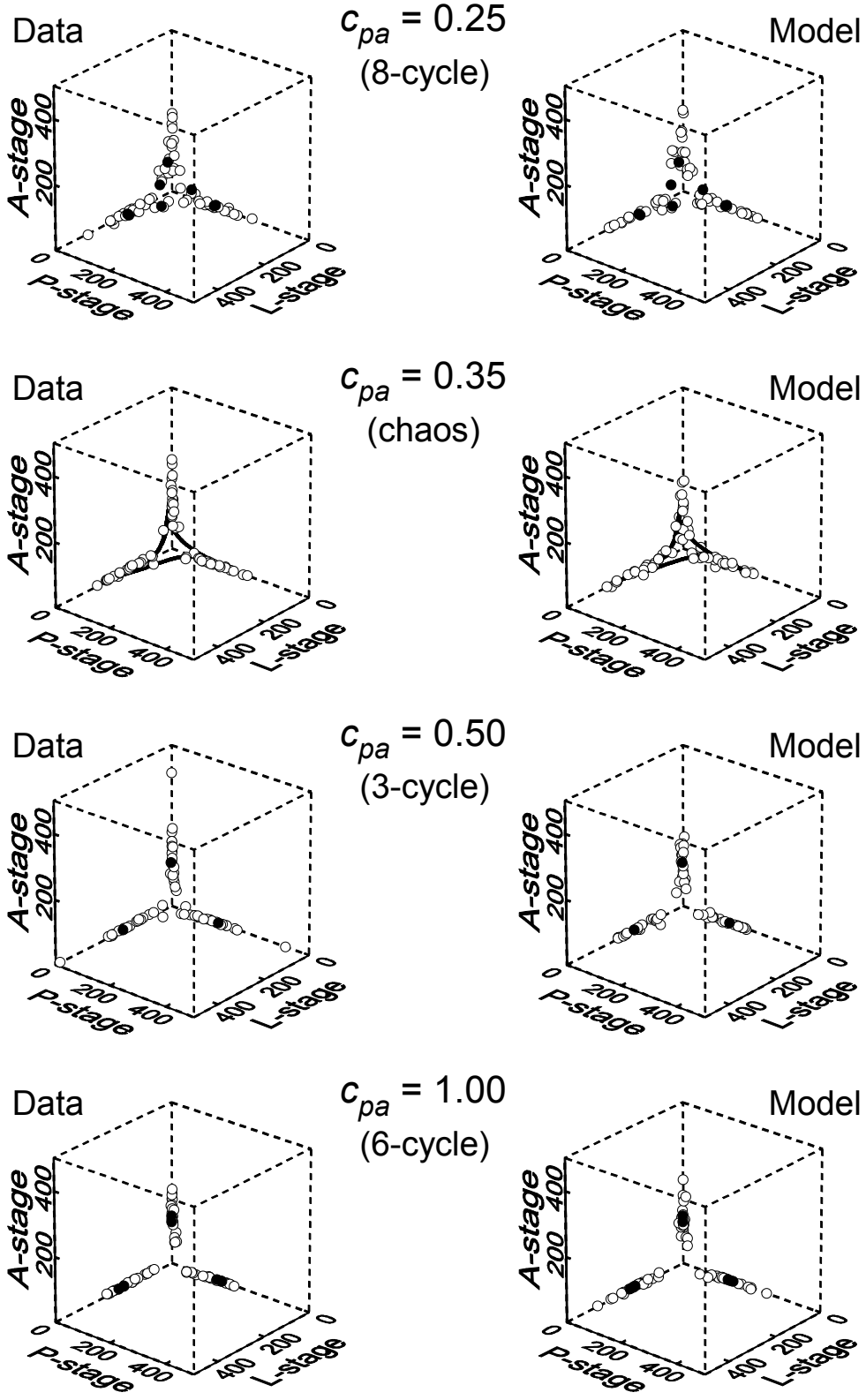
Data
c_{pa} = 0.25
(8-cycle)
Model
Data
c_{pa} = 0.35
(chaos)
Model
Data
c_{pa} = 0.50
(3-cycle)
Model
Data
c_{pa} = 1.00
(6-cycle)
Model
A-stage
P-stage
L-stage
0
200
400

Figure 5 (pt. 2)

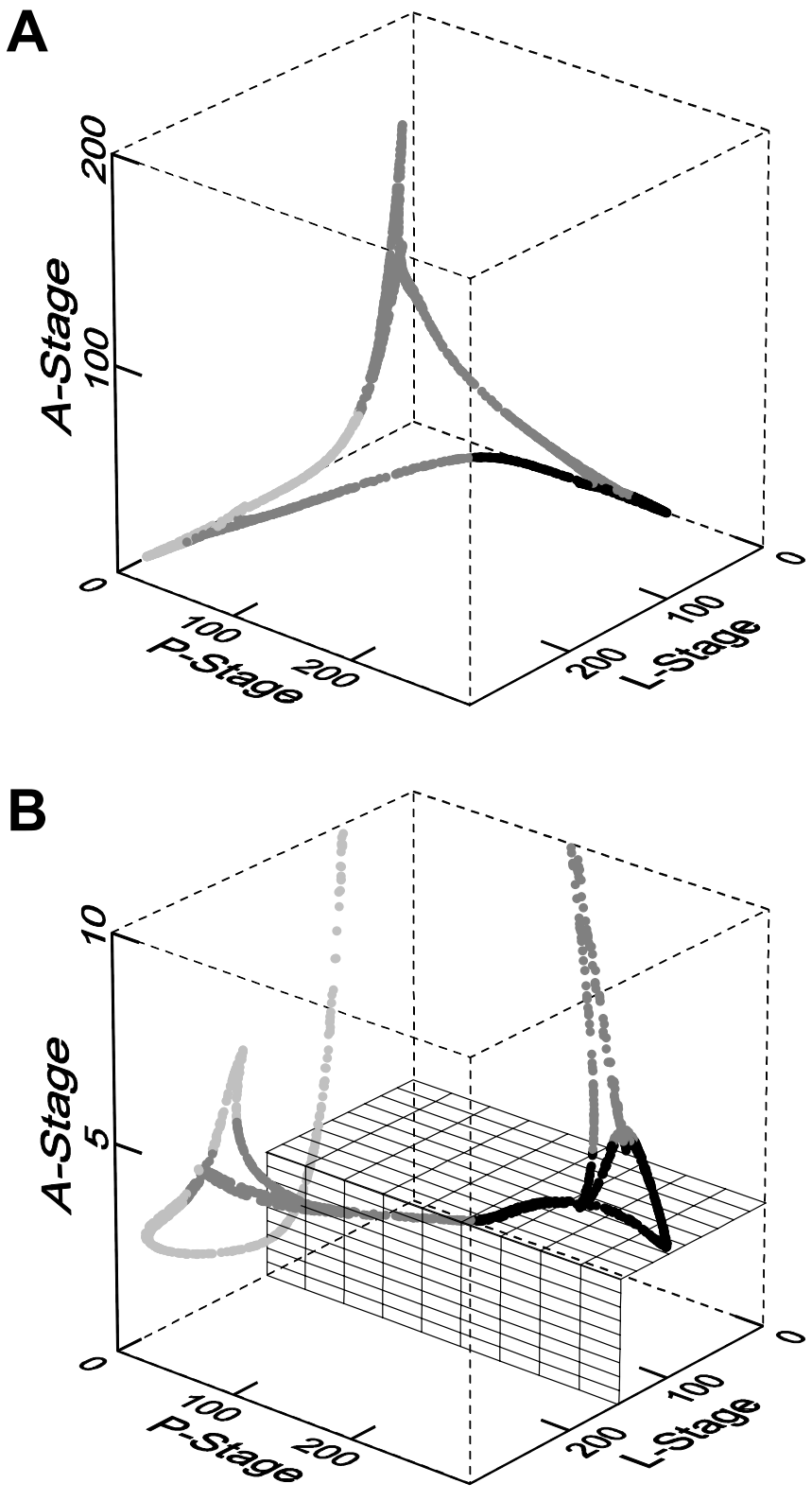
A
A-Stage
200
100
0
0
100
200
P-Stage
200
100
0
L-Stage
B
A-Stage
10
5
0
0
100
200
P-Stage
200
100
0
L-Stage

Figure 6

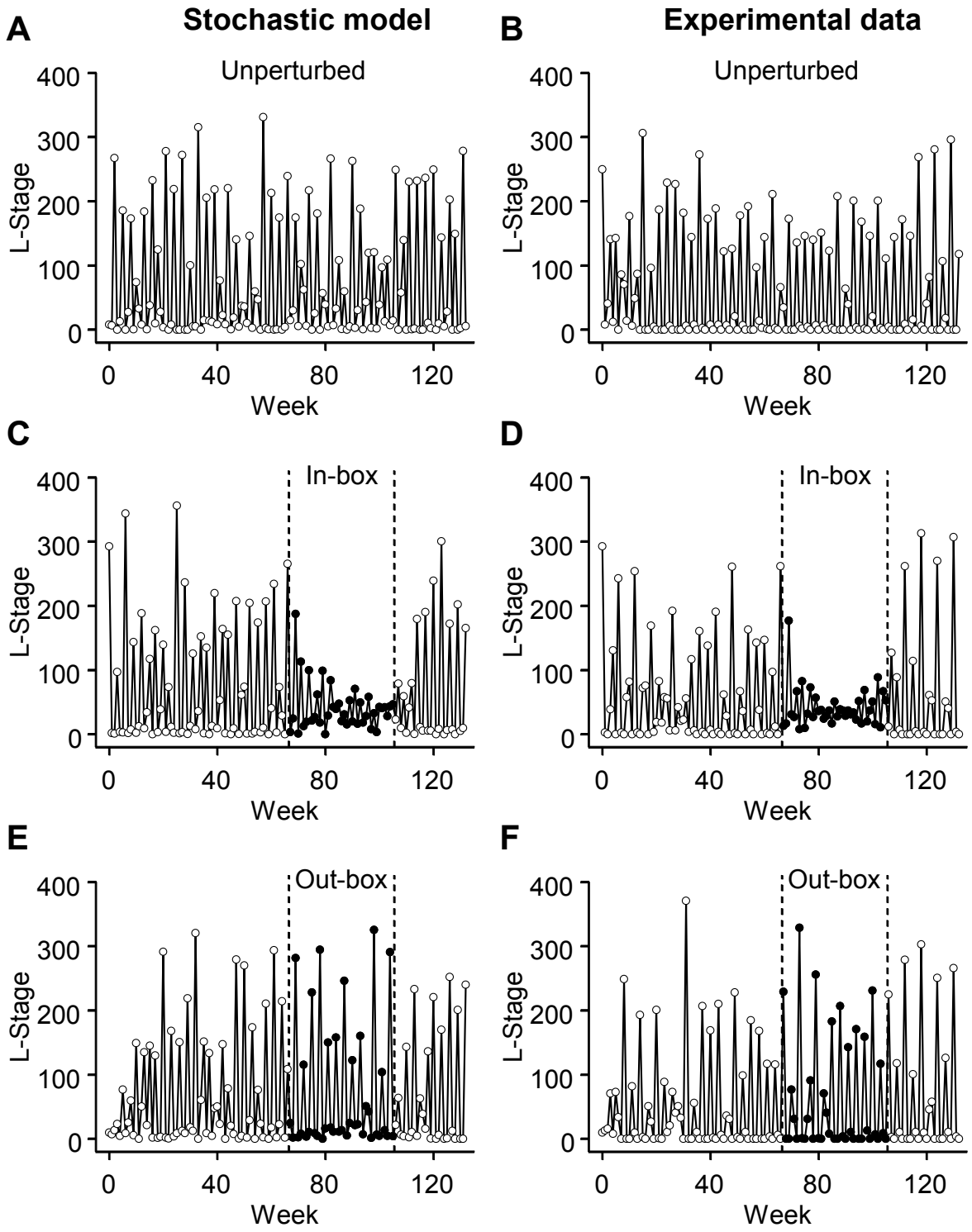
A
Stochastic model
Unperturbed
B
Experimental data
Unperturbed
C
In-box
D
In-box
E
Out-box
F
Out-box
L-Stage
Week
0
100
200
300
400
0
40
80
120

Figure 7

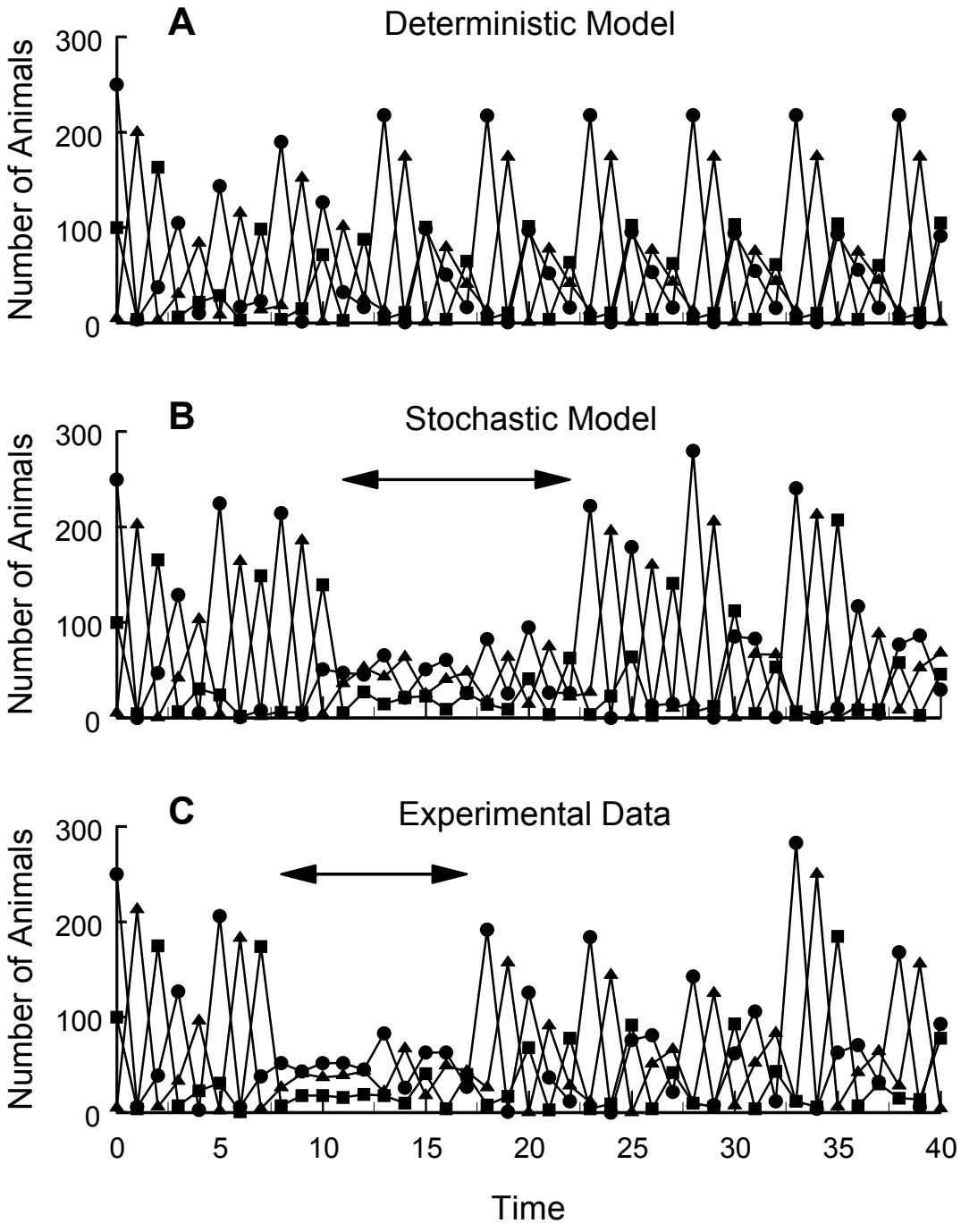
A
Deterministic Model
Number of Animals
300
200
100
0
B
Stochastic Model
Number of Animals
300
200
100
0
C
Experimental Data
Number of Animals
300
200
100
0
0
5
10
15
20
25
30
35
40
Time

Figure 8

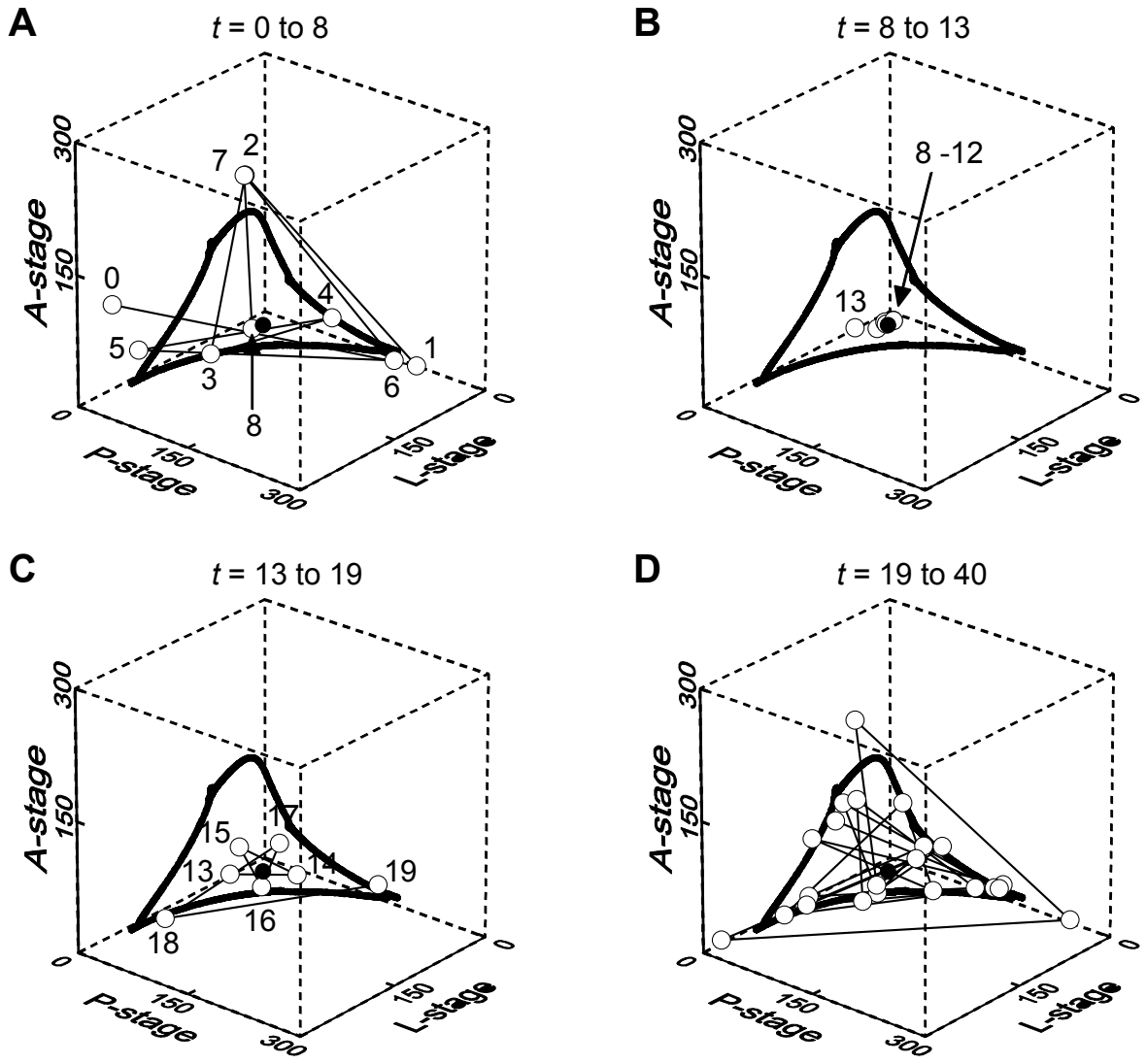
A
t = 0 to 8
A-stage
P-stage
L-stage
0
150
300
7
2
0
4
5
1
3
6
8
B
t = 8 to 13
8 -12
13
C
t = 13 to 19
15
17
13
14
19
16
18
D
t = 19 to 40

Figure 9

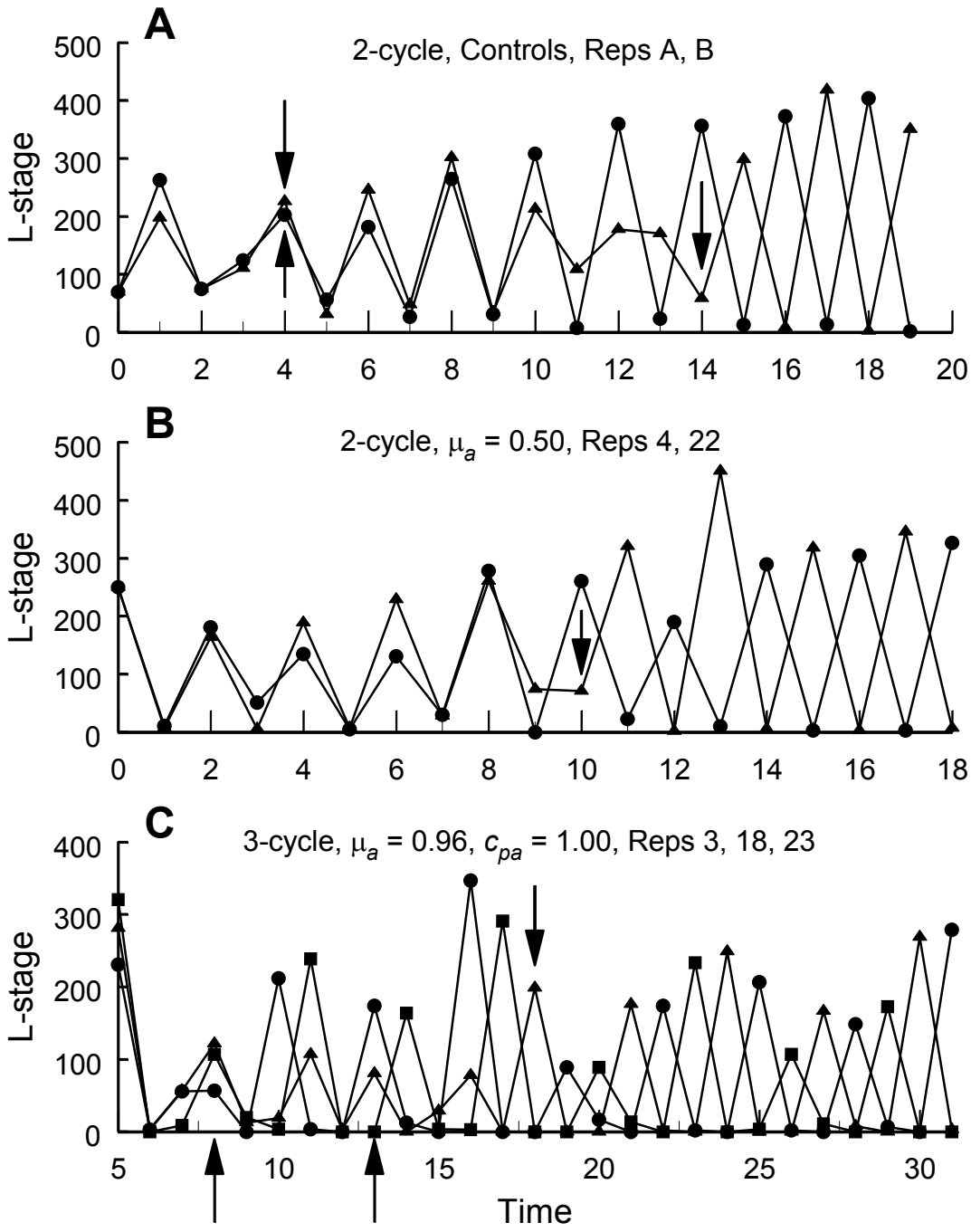
A
2-cycle, Controls, Reps A, B
L-stage
500
400
300
200
100
0
0
2
4
6
8
10
12
14
16
18
20
B
2-cycle, μ_a = 0.50, Reps 4, 22
L-stage
500
400
300
200
100
0
0
2
4
6
8
10
12
14
16
18
C
3-cycle, μ_a = 0.96, c_{pa} = 1.00, Reps 3, 18, 23
L-stage
400
300
200
100
0
5
10
15
20
25
30
Time

Figure 10

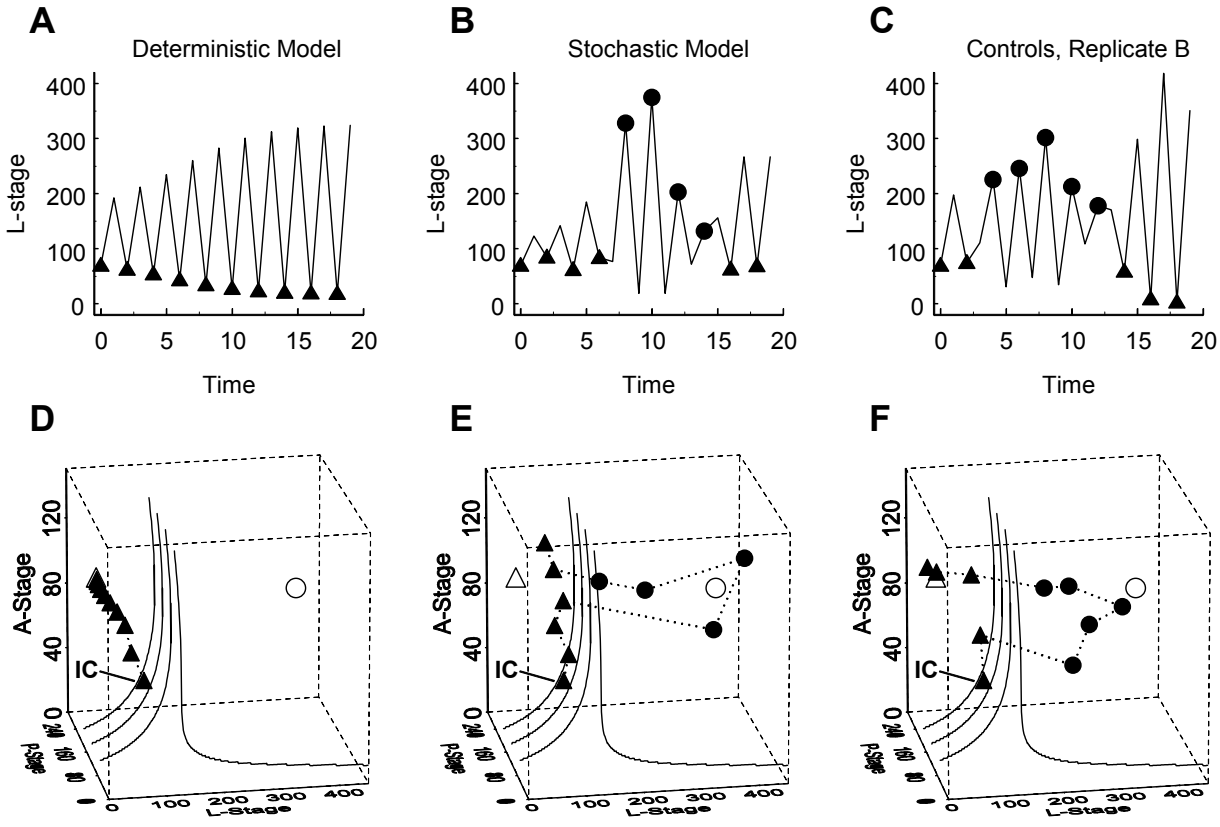
A
Deterministic Model
L-stage
Time
B
Stochastic Model
L-stage
Time
C
Controls, Replicate B
L-stage
Time
D
A-Stage
L-Stage
IC
E
A-Stage
L-Stage
IC
F
A-Stage
L-Stage
IC

Figure 11

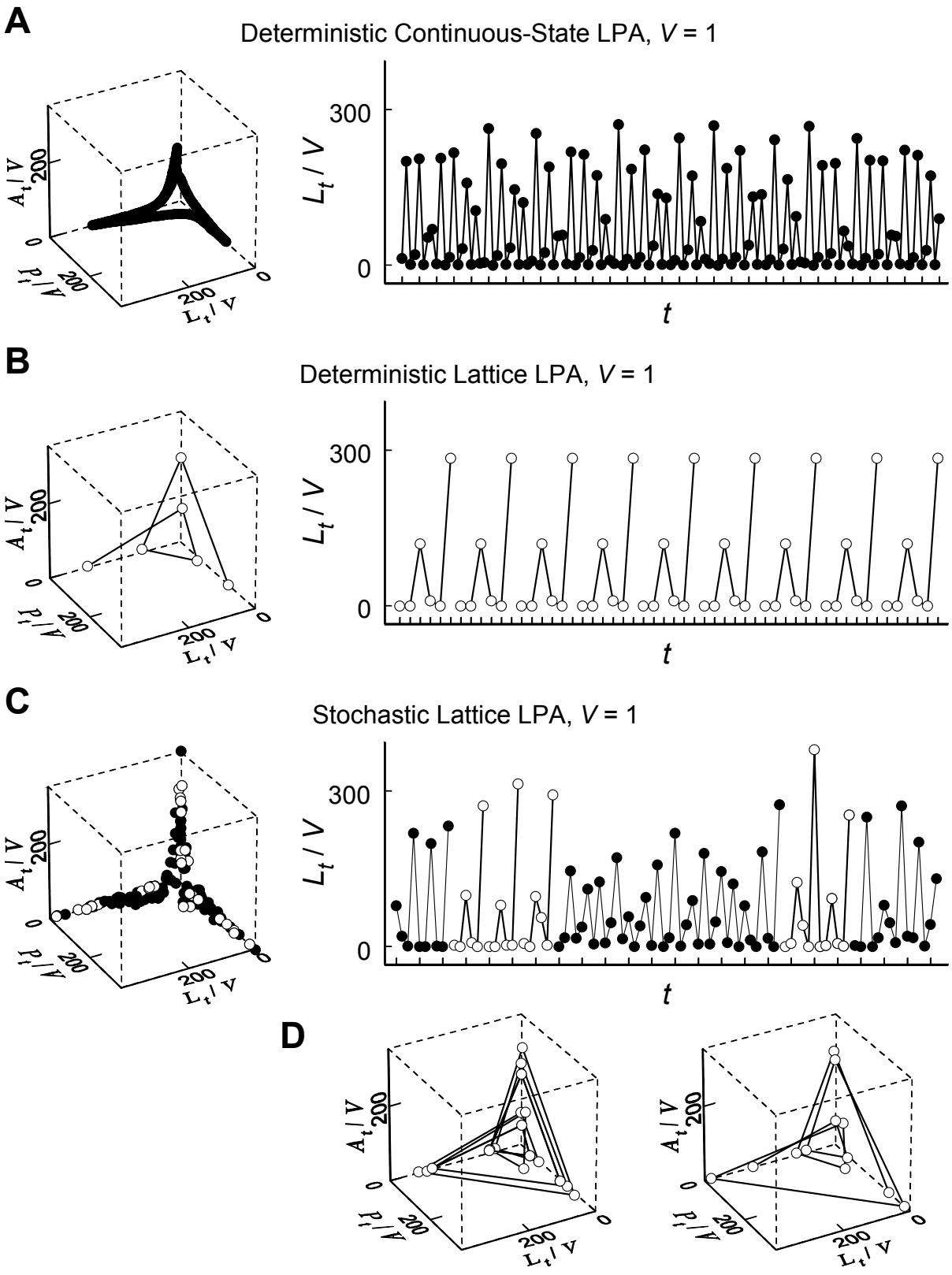
A
Deterministic Continuous-State LPA, V = 1
300
0
L_t / V
t
B
Deterministic Lattice LPA, V = 1
300
0
L_t / V
t
C
Stochastic Lattice LPA, V = 1
300
0
L_t / V
t
D
A_t / V
200
0
L_{t-1} / V
L_t / V

Figure 12

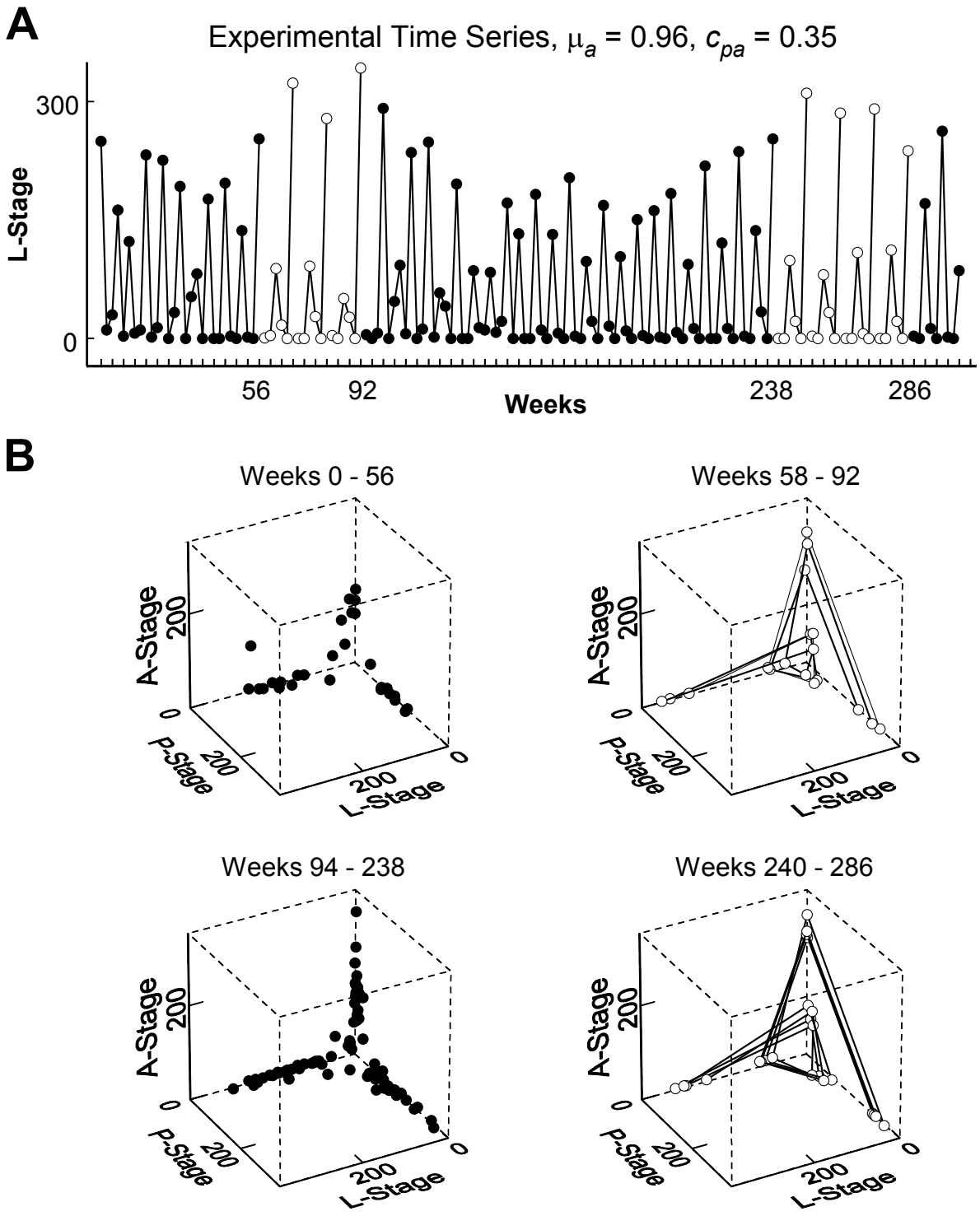
A
Experimental Time Series, μ_a = 0.96, c_{pa} = 0.35
300
0
L-Stage
56
92
Weeks
238
286
B
Weeks 0 - 56
Weeks 58 - 92
Weeks 94 - 238
Weeks 240 - 286
A-Stage
P-Stage
L-Stage
200
0

Figure 13

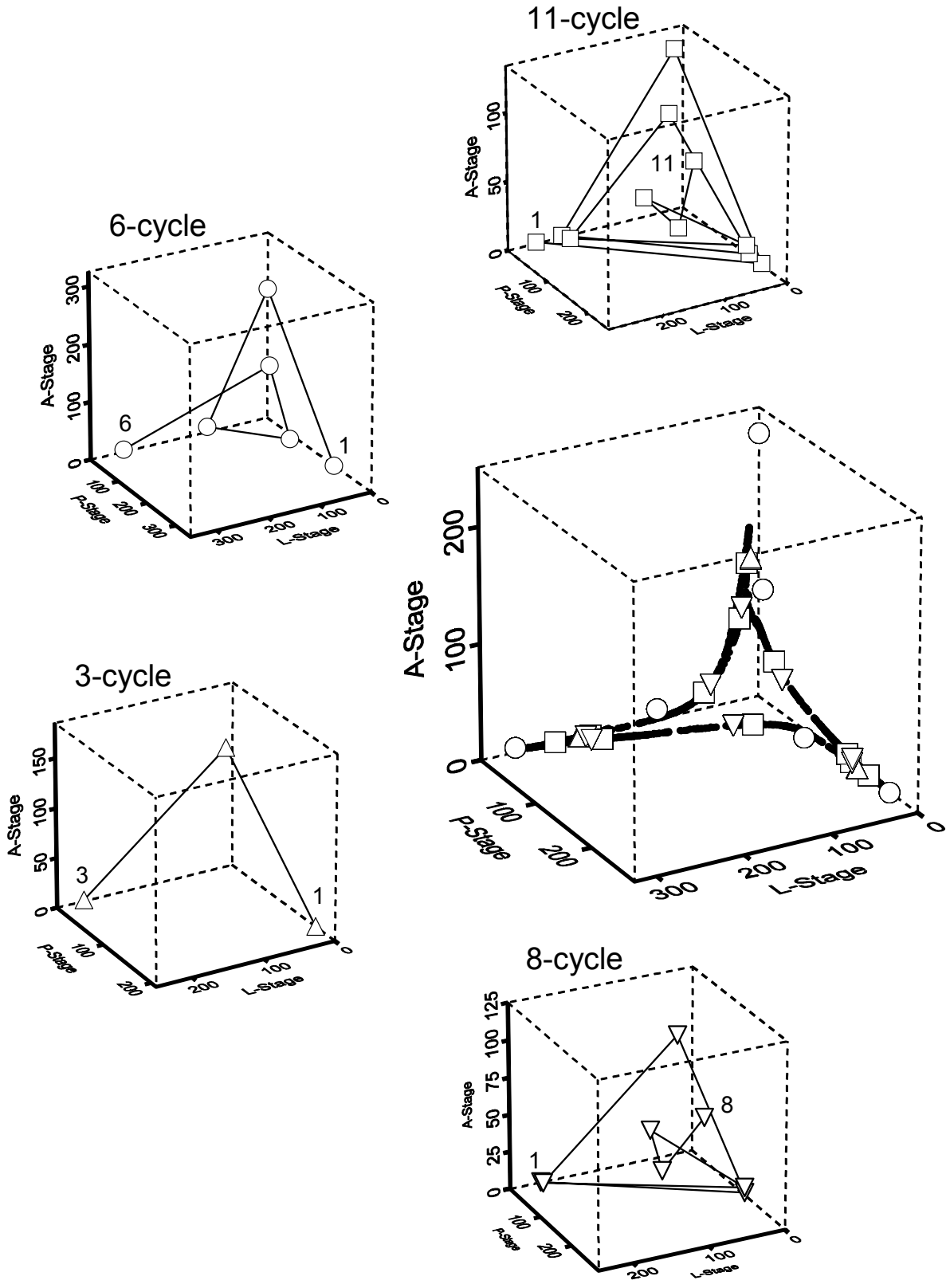
11-cycle
A-Stage
P-Stage
L-Stage
1
11
6-cycle
6
1
3-cycle
3
1
8-cycle
8
1

Figure 14

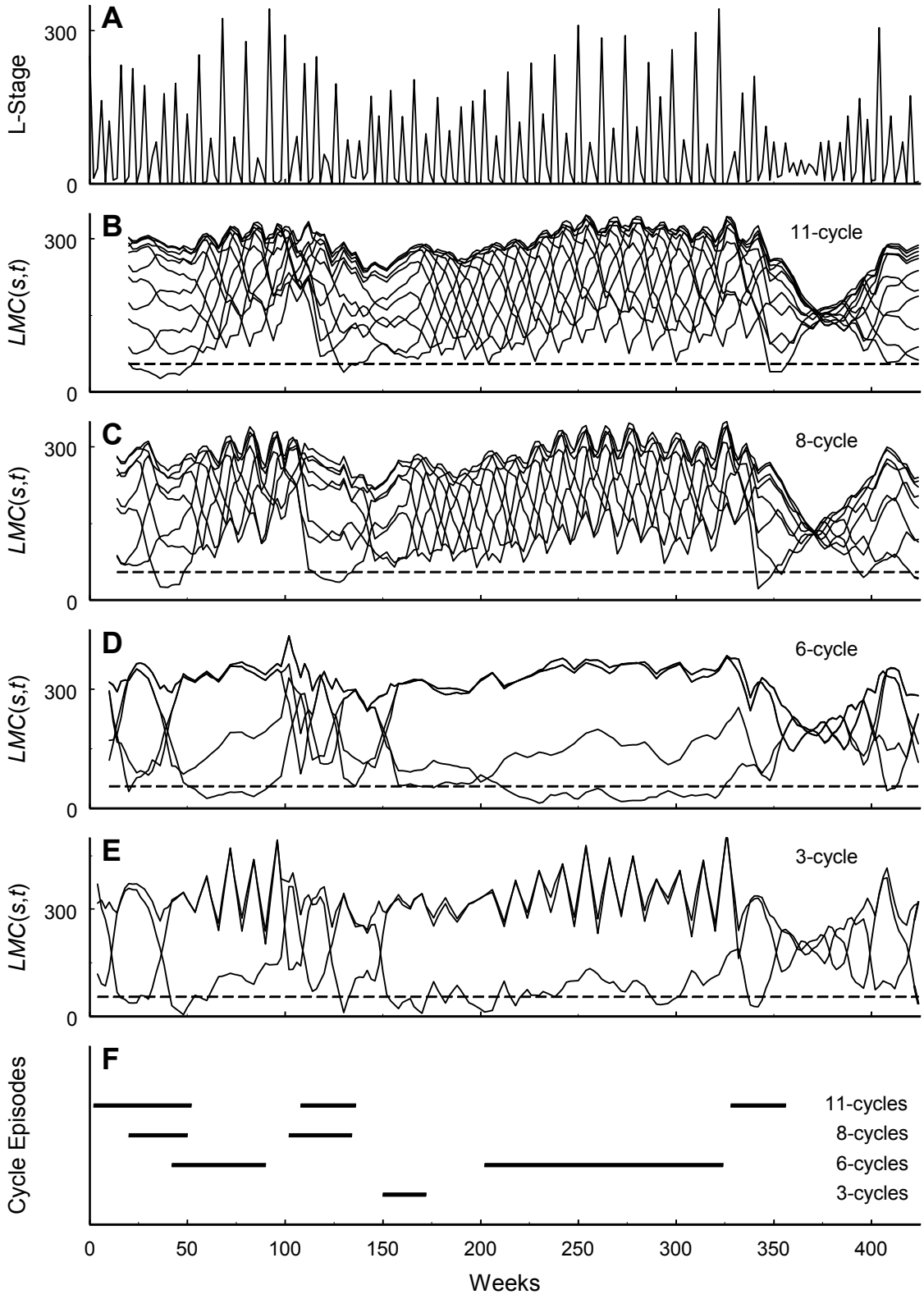
A
L-Stage
300
0
B
11-cycle
LMC(s,t)
C
8-cycle
D
6-cycle
E
3-cycle
F
Cycle Episodes
11-cycles
8-cycles
6-cycles
3-cycles
0
50
100
150
200
250
300
350
400
Weeks

Figure 15